Journal of Nonlinear Modeling and Analysis
Volume 7, Number 5, October 2025, 1830–1858
https://journal.global-sci.org/jnma
DOI:10.12150/jnma.2025.1830

Optimal Control Strategies for Reducing Toxic Formation in Acetaminophen Metabolism

Naurah Zahwa[1], Kasbawati[1,†] and Syamsuddin Toaha[1]

Abstract Acetaminophen (N-acetyl-para-aminophenol) is the most widely used painkiller in the world. Consuming acetaminophen involves a complex metabolic system, since it is converted into non-toxic and toxic metabolites called N-acetyl-p-benzoquinone imine (NAPQI). Acetaminophen is metabolized through a series of complex metabolic processes in the liver that involve enzymes as catalysts. This study presents a metabolic analysis of acetaminophen metabolism and its optimal regulation to reduce toxin formation. The metabolic study uses kinetic modeling combined with metabolic control analysis to identify key enzymes that can be modified to reduce hepatotoxicity due to excessive drug consumption. The sensitivity result shows that cytochrome (CYP) and uridine 5'-diphosphate-glucuronosyltransferase (UGT) are the two key enzymes that can be considered as internal control parameters. By inhibiting the reaction rate of CYP and UGT, the formation of N-acetyl-p-benzoquinone imine (NAPQI) can be reduced up to 69.9%, and the formation of Acetaminophen-Glucuronide (APAP-G) can be increased by approximately 0.49% such that Acetaminophen in the liver (APAP-L) can be excreted directly into the urine. Increasing the concentration of antioxidant GSH can also prevent hepatotoxicity by forming the complex NAPQI-GSH so that hepatotoxicity due to overconsumption of acetaminophen can be reduced.

Keywords Acetaminophen, hepatotoxicity, kinetic model, metabolic control analysis, optimal control theory

MSC(2010) 37N35, 35Q92, 92C45, 80M50.

1. Introduction

Acetaminophen, N-acetyl-para-aminophenol (APAP), often called paracetamol, is commonly used to relieve pain and fever [1]. Fever is very uncomfortable, as it usually comes with chills, nausea, headache, abdominal pain, and stomach discomfort [2]. APAP is a class of non-steroidal analgesic drugs that are safe when taken in recommended doses [3]. However, an overdose of acetaminophen can cause severe liver damage, and the extent of hepatocyte damage in patients with APAP overdose depends on the trade-off between induction and inhibition of CYP enzymes [4]. In 2015, the Australian Poison Control Center (PCC) reported receiving 13,322 calls explicitly related to acetaminophen incidents [5]. In the UK, 82,000 to 90,000 are admitted to the hospital due to an overdose of acetaminophen each year, and approximately 150-250 patients die [6].

[†]the corresponding author.
Email address:kasbawati@unhas.ac.id
[1]Applied Mathematics Laboratory, Department of Mathematics, Hasanuddin University, Indonesia

Acetaminophen involves a series of metabolic processes in the liver by interacting with enzymes. The metabolism process consists of various metabolic pathways that transform one compound into another in several stages. A specific enzyme guides each stage within this pathway. The metabolic system is essential to determine which compounds are nutrients and which are toxic to the body. Furthermore, acetaminophen metabolism occurs primarily in the liver through three main pathways: glucuronidation, sulfation, and oxidation. The glucuronidation and sulfation pathways are responsible for most acetaminophen detoxification, converting acetaminophen into water-soluble forms for excretion via urine. However, the oxidation pathway, mediated by the cytochrome P450 enzyme, produces a metabolite known as NAPQI (N-acetyl-p-benzoquinone imine). Although NAPQI is normally neutralized by conjugation with glutathione (GSH), excessive production can lead to glutathione depletion, resulting in cell damage and toxicity.

Modeling of acetaminophen metabolism has become an attraction in recent years. Reed et al. [7] studied the association of Michaelis-Menten's kinetics with acetaminophen metabolism through glucuronidation and sulfurization pathways. They used 20 blood and urine samples from patients who took acetaminophen at a dose of 60 mg/kg and 90 mg/kg. Reith et al. [8] also investigated Michaelis-Menten acetaminophen kinetics with the glucuronidation and sulfate pathways. The constructed model is a system of differential equations with fourteen variables related to the patient data. Other researchers have also built a model of the acetaminophen metabolism in the liver. In 2012, based on experimental data, Ben-Shachar et al. [9] formed an acetaminophen metabolism model with intestines, plasma, liver, tissue, and urine compartments. Predictions of death or recovery of patients were obtained depending on the extent of APAP overdose and the length of treatment. The model showed the effects of various acetaminophen doses on liver metabolism. Ramien et al. [10] also constructed a model of acetaminophen metabolism by studying acute liver damage caused by acetaminophen, then tested it on 53 patients at the University of Utah. Their research presented a method that could estimate the number of overdoses, the time since the start of overdose, and the probability of a patient's survival. The construction of the model involves the hepatocyte, APAP, glutathione, International Normalized Ratio (INR), aminotransferase (AST), and dynamics aspartate aminotransferase (ALT). Furthermore, Reddyhoff et al. [11] constructed a simpler mathematical model of acetaminophen metabolism by studying the time scale of the model. Their research was presented in a cell-based model. Their acetaminophen metabolism models in the liver compartment include cytochrome, sulfate, glucuronidation, glutathione, toxic metabolite production, and liver damage. With excessive doses of acetaminophen, the amount of glutathione S-transferase (GST) within liver cells became depleted, leading to N-acetyl-p-benzoquinone imine (NAPQI), which can not be bound by the antioxidant GSH. Their results showed that a high concentration of NAPQI binds with the living cells in the liver, ultimately causing liver damage [11,12]. Therefore, hepatotoxicity is minimal or absent as long as hepatic glutathione (GSH) is adequate for conjugation. However, over time, the depletion of hepatic GSH exceeds its regeneration rate, leading to the accumulation of reactive and toxic metabolites [13]. Hepatotoxicity is observed with the increased production of NAPQI when glutathione is depleted by approximately 70% [14]. Among these studies, a complete modeling of the enzymes involved in the acetaminophen pathway has not yet been considered. Due to the crucial role of enzymes in controlling the metabolic process, in this

study, we complete the modeling of acetaminophen metabolism by approximating all enzymatic processes using enzyme kinetics and studying their sensitivity. Our mathematical model is constructed by considering the model of Ben-Shachar et al. [9] and improving the kinetic model to approach the fundamental characteristics of all enzymes. The metabolite pathway is focused on the liver pathway [15] since an overdose of acetaminophen can probably be prevented by controlling the enzymes involved in the liver pathway [16]. Sensitivity analysis is conducted using the metabolic control analysis method to determine the level of sensitivity of the enzymes to the glutathione antioxidant in reducing the toxicity effects of acetaminophen. We believe that the level of enzyme sensitivity to model parameters can be used to control the hepatoxicity effect of acetaminophen. The sensitivity results are then used to determine optimal strategies that can maximize the production of antioxidant glutathione to reduce the toxicity of acetaminophen.

This paper is organized into several sections. In Section 2, we formulate the kinetic model based on the properties of acetaminophen metabolism. Section 3 presents the model analysis, including the model stability and sensitivity analysis using metabolic control analysis. Section 4 performs the formulation of the optimal control model and determines the necessary conditions for the optimality of the system. Section 5 presents some numerical simulations to clarify the analysis results and to study the effects of some control strategies on the reduction of the toxic metabolite. Finally, in Section 6, we summarize the essential findings and discuss potential directions for future research.

2. Model formulation

The kinetic model is formulated based on the liver metabolism pathway that acts as a functional organ, as seen in Figure 1. This pathway is also considered by [9].

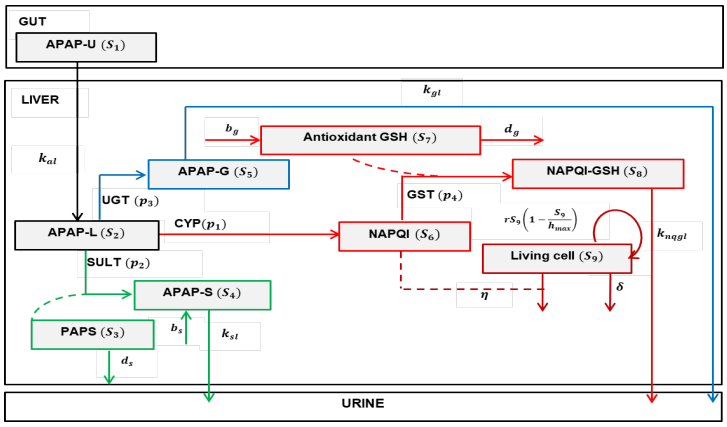

Figure 1. Schematic representation of acetaminophen metabolism in the liver. The considered variables are: 1. Acetaminophen (APAP) in gut (APAP-U); 2. APAP in the liver (APAP-U); 3. Phosphoadenosine-5'-phosphosulfate (PAPS) in the liver; 4. APAP Sulfate (APAP-S) in liver; 5. APAP Glucuronidate (APAP-G) in liver; 6. NAPQI in the liver; 7. Antioxidant GSH in the liver; 8. NAPQI-GSH in liver; 9. Living cells in the liver. The reactions are catalyzed by the following enzymes: p_1: Cytochrome (CYP); p_2: sulfotransferase (SULT); p_3: uridine 5'-diphospho-glucuronosyltransferase (UGT); p_4: glutathione S-transferase (GST). The solid lines represent reaction processes, and the dashed lines represent metabolite interaction.

Based on Figure 1, the concentration of APAP in the gut (S_1) is the concentration of acetaminophen introduced from the gut to the liver to be metabolized by the liver. The parameter k_{al} expresses the rate of APAP input from the gut to the liver. When APAP from the gut enters the liver, the concentration of APAP in the liver is metabolized through three main pathways: the cytochrome pathway (red line), the sulfation pathway (green line), and the glucuronidation pathway (blue line).

In the cytochrome pathway, acetaminophen is catalyzed by the cytochrome enzyme CYP (p_1). The process involves three cytochrome oxidases: CYP1A2, CYP2E1, and CYP3A4 [9]. Here, we model the three reactions using the Michaelis-Menten kinetic rate with irreversible mechanisms and Hill kinetic with cooperativity effects of the enzymes, such that the kinetic model on [9] becomes

$$p_1 = \left(\frac{V_1 S_2(t)}{K_{m1} + S_2(t)} + \frac{V_2 S_2(t)}{K_{m2} + S_2(t)} + \frac{V_3 S_2(t)}{K_{m3} + S_2(t)} \right) \left(1 + \frac{P(S_2(t))^n}{d^n + S_2(t)^n} \right), \quad (2.1)$$

where P and $V_i, i = 1 \cdots 3$, are the maximum rate of cytochrome oxidases enzymes, $K_{mj}, j = 1 \cdots 3$, and d are the Michaelis-Menten's constant, and n is the cooperativity coeffeicient, with $n > 1$. In the sulfation pathway, acetaminophen is catalyzed by an enzyme called sulfotransferase, SULT (p_2). Since the enzyme-catalyzed reaction involves two substrates, APAP-L and 3'-phosphoadenosine-5'-phosphosulfate (PAPS), and produces two products, acetaminophen sulfate (APAP-S) and 3'-phosphoadenosine-5'-phosphate (PAP), then we use "Bi-Bi" Michaelis-Menten kinetic for the irreversible mechanism [17] given by

$$p_2 = \frac{V_4 S_2(t) S_3(t)}{k_{\text{slt}} + K_{m4} S_2(t) + K_{m5} S_3(t) + S_2(t) S_3(t)}, \quad (2.2)$$

where V_4 is the maximum rate of SULT and K_{m4} and K_{m5} are the Michaelis-Menten's constant of SULT. PAP is the residual product of the sulfate donor, which can be recycled or further broken down in the cell (it is not considered in this modeling process). The enzyme sulfotransferase (SULT) catalyzes the transfer of the sulfate group (sulfation) from 3'-phosphoadenosine-5'-phosphosulfate (PAPS). PAPS is the universal sulfate donor in sulfation reactions in the body. PAPS supplies the sulfate groups required for reactions catalyzed by SULT. PAPS is formed from adenosine triphosphate (ATP) and inorganic sulfate (SO_4^{2-}) through several enzymatic steps.

The result of APAP catalyzed by sulfation forms the APAP Sulfate reaction (APAP-S). This product is the sulfated form of APAP. APAP-S is a more water-soluble metabolite than APAP, which is more easily excreted through urine. The rate $k_{\text{sl}} S_4$ expresses the rate of output of APAP Sulfate into the urine. The concentration of APAP-S is increased by natural production in the liver with the rate of sulfate production b_s.

Similarly, the glucuronidation pathway is catalyzed by uridine 5'-diphosphate-glucuronosyltransferase, UGT (p_3), to form the APAP Glucuronidate (APAP-G) that will be excreted from the liver and transferred to the urine with the rate $k_{\text{gl}} S_5$. Uridine 5'-diphosphate-glucuronosyltransferase and sulfotransferase form products that do not harm cells [18]. There are four glucuronosyltransferase that glucuronidated APAP, i.e., UGT1A6, modeled using Michaelis-Menten kinetic; UGT2B15, modeled using Hill kinetic; UGT1A1 and UGT1A9, modeled using

Michaelis-Menten kinetics with substrate inhibition as follows [9]

$$p_3 = \frac{V_5(S_2)^m}{(K_{m6})^m + (S_2)^m} + \frac{V_6 S_2}{K_{m7} + S_2(1 + S_2/K_{i7})} + \frac{V_7 S_2}{K_{m8} + S_2} + \frac{V_8 S_2}{K_{m9} + S_2(1 + S_2/K_{i9})}, \tag{2.3}$$

where V_i, $i = 5 \cdots 8$, are the maximum rate of UGT, K_{mj} , $j = 6 \cdots 9$, are the Michaelis-Menten's constant, K_{i7} and K_{i9} are constants of inhibition, and m is cooperativity. In the cytochrome pathway, NAPQI is highly reactive and causes cell death if it is not neutralized promptly. Detoxification of NAPQI involves glutathione (GSH) and the enzyme glutathione S-transferase, GST (p_4), as catalysts. GST catalyzes the conjugation reaction between NAPQI and GSH, producing a more stable and less toxic compound, NAPQI-glutathione (NAPQI-GSH) conjugate. The detoxification reaction is irreversible and involves two substrates, resulting in one product that is modeled as follows

$$p_4 = \frac{V_9 S_6(t) S_7(t)}{k_{\text{gsh}} + K_{m10} S_6(t) + K_{m11} S_7(t) + S_6(t) S_7(t)}, \tag{2.4}$$

where V_9 is the maximum rate of GST, K_{m10} and K_{m11} are the constants of Michaelis-Menten. Additionally, GSH concentration naturally decreases at a rate $d_g S_6$ as a parameter. GSH concentration increases with the GSH natural production rate b_g. Furthermore, NAPQI-GSH is excreted through urine [19] with excretion rate $k_{\text{nqgl}} S_8$. The concentration of NAPQI-GSH in the liver is more water-soluble and less reactive than NAPQI. This conjugate can undergo the NAPQI-GSH reaction. This compound is a detoxification product.

A similar process occurs in the detoxification of NAPQI catalyzed by glutathione. Liver cells reproduce substances in the liver, such as bile, repair red blood cells, store energy reserves, regulate immunity, and detoxify NAPQI. Cells die due to toxicity in acetaminophen metabolism at a rate of $\eta S_6 S_9$, and cells also naturally die at a rate of δS_9. Liver damage occurs due to the excessive production of NAPQI, which cannot be bound by the antioxidant GSH, and thus damages living cells. Based on the assumptions, we formulate the rate of the changes of each metabolite that can be written mathematically as follows

$$\begin{aligned}
\dot{S}_1 &= -k_{al} S_1(t), \\
\dot{S}_2 &= k_{al} S_1(t) - p_1 - p_2 - p_3, \\
\dot{S}_3 &= -p_2 - d_s S_3, \\
\dot{S}_4 &= p_2 + b_s - k_{sl} S_4, \\
\dot{S}_5 &= p_3 - k_{gl} S_5, \\
\dot{S}_6 &= p_1 - p_4 - \eta S_6 S_9, \\
\dot{S}_7 &= -p_4 + b_g - d_g S_7, \\
\dot{S}_8 &= p_4 - k_{nqgl} S_8, \\
\dot{S}_9 &= r S_9(t) \left(1 - \frac{S_9(t)}{h_{\max}}\right) - \eta S_6(t) S_9(t) - \delta S_9(t),
\end{aligned} \tag{2.5}$$

where $p_i, i = 1...4$ is given in equations (2.1)-(2.4). The initial conditions applied for system (2.5) are taken from [9], which are $S_1(0) = 7\mu M$, $S_2(0) = 4\ \mu M$, $S_3(0)$

$= 1\ \mu M$, $S_4(0) = 1\ \mu M$, $S_5(0) = 0\ \mu M$, $S_6(0) = 0\ \mu M$, $S_7(0) = 0.5\ \mu M$, $S_8(0) = 0\ \mu M$, and $S_9(0) = 0.2\ \mu M$. The description of each parameter is shown in Table 1.

Table 1. List of model parameters and its value.

Par	Value	Unit	Ref.	Par	Value	Unit	Ref.
k_{al}	4	h^{-1}	[9]	r	0.04	h^{-1}	[9]
K_{m9}	23000	μM	[38]	K_{m10}	15	μM	[35]
k_{gl}	0.81	h^{-1}	[9]	δ	0.08	h^{-1}	[9]
k_{sl}	0.24	h^{-1}	[9]	K_{m1}	3430	μM	[41]
K_{m11}	4600	μM	[42]	K_{i7}	23000	μM	[38]
k_{gsh}	1.87×10^{-3}	μM^2	[37]	K_{m2}	677	μM	[41]
k_{nqgl}	0.29	h^{-1}	[9]	K_{m3}	276	μM	[41]
K_{i9}	5300	μM	[38]	P	20		[9]
k_{slt}	13.27	μM^2	[9]	K_{m4}	97	μM	[8]
b_g	0.07	μM.h^{-1}	[10]	K_{m5}	3.3×10^{-3}	μM	[39]
d	18000	μM	[9]	n	2		[9]
m	3		[9]	h_{max}	1.6×10^{11}	μM	[10]
d_g	0.08	h^{-1}	[34, 36, 40]	K_{m6}	5500	μM	[38]
d_s	0.08	h^{-1}	[34, 36, 40]	K_{m7}	4000	μM	[38]
b_s	0.13	μM.h^{-1}	[10]	K_{m8}	9200	μM	[38]
V_1	0.55	μM.h^{-1}	[41]	V_2	345	μM.h^{-1}	[41]
V_3	0.99	μM.h^{-1}	[41]	V_6	490	μM.h^{-1}	[38]
V_4	1785	μM.h^{-1}	[39]	V_5	6370	μM.h^{-1}	[38]
V_7	4900	μM.h^{-1}	[38]	V_8	8820	μM.h^{-1}	[38]
η	0.21×10^{-4}	μM^{-1}.h^{-1}	[9]	V_9	72000	μM.h^{-1}	[42]

3. Model analysis

In this section, we study the local stability of the system (2.5) by first finding the conditions for the existence of its positive steady-state solutions. The results are then used to examine how sensitive the reaction rate and metabolite flux distribution are within the pathways, such that we can reveal how liver metabolic changes in parameters can significantly impact the steady-state properties of the system.

3.1. Stability analysis of the positive steady-state solution

A steady-state solution is obtained by taking the right-hand side of the system (2.5) equal to zero. If we assume the steady state is x_E, then we get

$$x_E = (0, S_2^*, S_3^*, S_4^*, S_5^*, S_6^*, S_7^*, S_8^*, S_9^*), \tag{3.1}$$

where

$$S_3^* = \frac{S_2^* V_4 - d_s(K_{m4} S_2^* + k_{slt})}{d_s(K_{m5} + S_2^*)}, \quad \text{that is positive iff} \quad S_2^* V_4 > d_s(K_{m4} S_2^* + k_{slt}),$$

$$
\begin{aligned}
S_4^* =& \frac{K_{m4}S_2^*b_s + K_{m5}S_3^*b_s + S_2^*S_3^*V_4 + S_2^*S_3^*b_s + b_sk_{slt}}{(K_{m4}S_2^* + K_{m5}S_3^* + S_2^*S_3^* + k_{slt})k_{sl}} > 0,\\
S_5^* =& S_2^*\Big((V_5+V_7)S_2^{*7} + \Big((V_5+V_6+V_7)K_{i7} + (V_5+V_7+V_8)K_{i9} + K_{m8}V_5\Big)S_2^{*6}\\
&+ \Big(\big((V_5+V_6+V_7+V_8)K_{i9} + (V_5+V_6)K_{m8} + K_{m7}(V_5+V_7)\big)K_{i7} + K_{i9}((V_5\\
&+ V_8)K_{m8} + K_{m9}(V_5+V_7))\Big)S_2^{*5} + \Big(\big(((V_5+V_6+V_8)K_{m8} + (V_5+V_7+V_8)K_{m7}\\
&+ K_{m9}(V_5+V_6+V_7)\big)K_{i9} + K_{m7}K_{m8}V_5\big)K_{i7} + K_{m8}K_{m9}V_5K_{i9} + K_{m6}^3V_7\Big)S_2^{*4} +\\
&+ \Big(\big(\big(((V_5+V_8)K_{m7} + K_{m9}(V_5+V_6)\big)K_{m8} + K_{m7}K_{m9}(V_5+V_7)\big)K_{i9} + K_{m6}^3(V_6\\
&+ V_7)\big)K_{i7} + K_{m6}^3(V_7+V_8)K_{i9}\Big)S_2^{*3} + \Big(\big(((V_6+V_7+V_8)K_{m6}^3 + K_{m7}K_{m8}K_{m9}\\
&V_5\big)K_{i9} + K_{m6}^3(K_{m7}V_7 + K_{m8}V_6)\big)K_{i7} + (K_{m8}V_8 + K_{m9}V_7)K_{m6}^3K_{i9}\Big)S_2^{*2} + \big((V_6\\
&+ V_8)K_{m8} + (V_7+V_8)K_{m7} + K_{m9}(V_6+V_7)\big)K_{i9}K_{i7}K_{m6}^3S_2^* + \big((K_{m7}V_8 + K_{m9}V_6)\\
&K_{m8} + K_{m7}K_{m9}V_7\big)K_{m6}^3K_{i7}K_{i9}\Big)/\Big(k_{gl}(S_2^* + K_{m6})(K_{i7}K_{m7} + K_{i7}S_2^* + S_2^{*2})(S_2^*\\
&+ K_{m8})(K_{i9}K_{m9} + K_{i9}S_2^* + S_2^{*2})[(K_{m6} - S_2^*)^2 + K_{m6}S_2^*]\Big) > 0,\\
S_8^* =& \frac{V_9S_6^*S_7^*}{(K_{m10}S_6^* + K_{m11}S_7^* + S_6^*S_7^* + k_{gsh})k_{nqgl}} > 0,\\
S_9^* =& \frac{h_{max}(r - (S_6^*\eta + \delta))}{r}, \quad \text{that is positive iff} \quad r > S_6^*\eta + \delta.
\end{aligned}
$$

The solutions of S_2, S_6 and S_7 can not be found explicitly. Therefore, the existence of their positive solutions will be discussed as follows. Substituting S_3^* into the second equation of (2.5) gives the zeros of S_2 in term of the roots of polynomial,

$$\mathcal{A}_1S_2^7 + \mathcal{A}_2S_2^6 + \mathcal{A}_3S_2^5 + \mathcal{A}_4S_2^4 + \mathcal{A}_5S_2^3 + \mathcal{A}_6S_2^2 + \mathcal{A}_7S_2 + \mathcal{A}_8 = 0, \tag{3.2}$$

where

$$
\begin{aligned}
\mathcal{A}_1 =& -(V_5+V_7) < 0,\\
\mathcal{A}_2 =& -(V_5+V_6+V_7)K_{i7} - (V_5+V_7+V_8)K_{i9} - K_{m8}V_5 < 0,\\
\mathcal{A}_3 =& -\big([V_5+V_6+V_7+V_8]K_{i9} + [V_5+V_6]K_{m8} + K_{m7}[V_5+V_7]\big)K_{i7} - K_{i9}\big([V_5\\
&+ V_8]K_{m8} + K_{m9}[V_5+V_7]\big) < 0,\\
\mathcal{A}_4 =& -(P+1)(V_1+V_2+V_3) - \big(([V_5+V_6+V_8]K_{m8} + [K_{m9}+K_{m7}]V_5 + [K_{m9}\\
&+ K_{m7}]V_7 + K_{m9}V_6 + V_8K_{m7})K_{i9} + K_{m8}V_5K_{m7}\big)K_{i7} - K_{m8}K_{m9}V_5K_{i9}\\
&- V_7K_{m6}^3 < 0,\\
\mathcal{A}_5 =& -(P+1)\Big((V_2+V_3)K_{m1} + [V_1+V_3]K_{m2} + K_{m3}[V_1+V_2]\Big)
\end{aligned}
$$

$$
\begin{aligned}
&- \Big(\big(\{V_5[K_{m9} + K_{m7}] + K_{m9}V_6 + V_8K_{m7}\}K_{m8} + K_{m9}K_{m7}[V_5 + V_7] \big) K_{i9} \\
&+ K_{m6}^3[V_6 + V_7] \Big) K_{i7} - K_{i9}K_{m6}^3[V_7 + V_8] < 0, \\
\mathcal{A}_6 = &- d^2(V_1 + V_2 + V_3) - (P+1)\left([K_{m2}V_3 + K_{m3}V_2]K_{m1} + K_{m2}K_{m3}V_1\right) - \big(\{[V_6 \\
&+ V_7 + V_8]K_{m6}^3 + K_{m8}K_{m9}V_5K_{m7}\}K_{i9} + K_{m6}^3[K_{m7}V_7 + K_{m8}V_6]\big)K_{i7} \\
&- K_{i9}K_{m6}^3[K_{m8}V_8 + K_{m9}V_7] < 0, \\
\mathcal{A}_7 = &- d^2\big([V_2 + V_3]K_{m1} + [V_1 + V_3]K_{m2} + K_{m3}[V_1 + V_2]\big) - (K_{m4}V_4d_s + V_4^2) \\
&- \big([V_6 + V_8]K_{m8} + (K_{m9} + K_{m7})V_7 + K_{m9}V_6 + V_8K_{m7}\big)K_{i7}K_{i9}K_{m6}^3 < 0, \\
\mathcal{A}_8 = &- d^2\big([K_{m2}V_3 + K_{m3}V_2]K_{m1} + K_{m2}K_{m3}V_1\big) + V_4d_sk_{slt} \\
&- K_{i7}K_{i9}\big([K_{m7}V_8 + K_{m9}V_6]K_{m8} + K_{m9}V_7K_{m7}\big)K_{m6}^3.
\end{aligned}
$$

The roots of (3.2) are challenging to find due to the complexity of the dependencies of its polynomial coefficients. Therefore, the positive roots of S_2 will be investigated using Descartes's rule of signs by [22]. Since $\mathcal{A}_1, \ldots, \mathcal{A}_7$ are negative for all positive parameters, the number of positive roots of (3.2) depends on the sign of $\mathcal{A}_8$. If $\mathcal{A}_8 > 0$, we get one sign change, meaning one positive root exists for S_2.

Furthermore, for S_6, substituting S_9^* into the sixth equation of (2.5), we get the zeros of S_6 in term of the roots of polynomial,

$$\mathcal{B}_1S_6^3 + \mathcal{B}_2S_6^2 + \mathcal{B}_3S_6 + \mathcal{B}_4 = 0, \tag{3.3}$$

where

$$
\begin{aligned}
\mathcal{B}_1 = &\delta h_{\max}\eta(K_{m10} + S_7^*)S_2^{*5} + \delta h_{\max}\eta(K_{m10} + S_7^*)(K_{m1} + K_{m2} + K_{m3})S_2^{*4} \\
&+ h_{\max}\big[(K_{m2} + K_{m3})K_{m1} + K_{m2}K_{m3} + d^2\big]\delta\eta(K_{m10} + S_7^*)S_2^{*3} \\
&+ h_{\max}\eta\big[(K_{m2}K_{m3} + d^2)K_{m1} + (K_{m2} + K_{m3})d^2\big]\delta(K_{m10} + S_7^*)S_2^{*2} \\
&+ (K_{m10} + S_7^*)\big[(K_{m2} + K_{m3})K_{m1} + K_{m2}K_{m3}\big]h_{\max}\delta\eta d^2S_2^* \\
&+ \delta h_{\max}\eta(K_{m10} + S_7^*)K_{m3}K_{m1}d^2K_{m2} > 0, \\
\mathcal{B}_2 = &h_{max}((-K_{m10} - S_7^*)r + (K_{m10} + S_7^*)\delta + \eta(K_{m11}S_7^* + k_{gsh}))\delta S_2^{*5} \\
&+ h_{max}((-K_{m10} - S_7^*)r + (K_{m10} + S_7^*)\delta + \eta(K_{m11}S_7^* + k_{gsh}))\delta(K_{m1} + K_{m2} \\
&+ K_{m3})S_2^{*4} + h_{max}((K_{m2} + K_{m3})K_{m1} + K_{m2}K_{m3} + d^2)((-K_{m10} - S_7^*)r \\
&+ (K_{m10} + S_7^*)\delta + \eta(K_{m11}S_7^* + k_{gsh}))\delta S_2^{*3} + h_{max}((-K_{m10} - S_7^*)r + (K_{m10} + S_7^*)\delta \\
&+ \eta(K_{m11}S_7^* + k_{gsh}))((K_{m2}K_{m3} + d^2)K_{m1} + (K_{m2} + K_{m3})d^2)\delta S_2^{*2} \\
&+ d^2h_{max}((-K_{m10} - S_7^*)r + (K_{m10} + S_7^*)\delta + \eta(K_{m11}S_7^* + k_{gsh})) \\
&\times \delta((K_{m2} + K_{m3})K_{m1} + K_{m2}K_{m3})S_2^* + d^2K_{m3}K_{m2}h_{max}((-K_{m10} - S_7^*)r \\
&+ (K_{m10} + S_7^*)\delta + \eta(K_{m11}S_7^* + k_{gsh}))\delta K_{m1}, \\
\mathcal{B}_4 = &r(K_{m11}S_7^* + k_{gsh})(V_3 + V_1 + V_2)(P+1)S_2^{*5} + (K_{m11}S_7^* + k_{gsh})((V_3 + V_2)K_{m1} \\
&+ (V_3 + V_1)K_{m2} + K_{m3}(V_1 + V_2))(P+1)rS_2^{*4} + (K_{m11}S_7^* + k_{gsh})((K_{m2}V_3 \\
&+ K_{m3}V_2)(P+1)K_{m1} + K_{m3}V_1(P+1)K_{m2} + d^2(V_3 + V_1 + V_2))rS_2^{*3} + (K_{m11}S_7^* \\
&+ k_{gsh})((V_3 + V_2)K_{m1} + (V_3 + V_1)K_{m2} + K_{m3}(V_1 + V_2))d^2rS_2^{*2} + d^2(K_{m11}S_7^* \\
&+ k_{gsh})((K_{m2}V_3 + K_{m3}V_2)K_{m1} + K_{m2}K_{m3}V_1)rS_2^* > 0,
\end{aligned}
$$

$$\begin{aligned}\mathcal{B}_3 = &((-\delta(K_{m11}S_7^* + k_{gsh})h_{max} + ((P+1)V_1 + (P+1)V_2 + (P+1)V_3 - V_9)S_7^* \\ &+ K_{m10}(V_3 + V_1 + V_2)(P+1))r + \delta^2 h_{max}(K_{m11}S_7^* + k_{gsh}))S_2^{*5} + ((-\delta(K_{m11}S_7^* \\ &+ k_{gsh})(K_{m1} + K_{m2} + K_{m3})h_{max} + (((P+1)V_2 + (P+1)V_3 - V_9)K_{m1} + ((P \\ &+ 1)V_1 + (P+1)V_3 - V_9)K_{m2} + K_{m3}((P+1)V_1 + (P+1)V_2 - V_9))S_7^* \\ &+ K_{m10}((V_3 + V_2)K_{m1} + (V_3 + V_1)K_{m2} + K_{m3}(V_1 + V_2))(P+1))r + \delta^2 h_{max}(K_{m11}S_7^* \\ &+ k_{gsh})(K_{m1} + K_{m2} + K_{m3}))S_2^{*4} + ((-(K_{m11}S_7^* + k_{gsh})((K_{m2} + K_{m3})K_{m1} \\ &+ K_{m2}K_{m3} + d^2)\delta h_{max} + ((((P+1)V_3 - V_9)K_{m2} + ((P+1)V_2 - V_9)K_{m3})K_{m1} \\ &+ K_{m3}((P+1)V_1 - V_9)K_{m2} + d^2(V_3 - V_9 + V_1 + V_2))S_7 + K_{m10}((K_{m2}V_3 \\ &+ K_{m3}V_2)(P+1)K_{m1} + K_{m3}V_1(P+1)K_{m2} + d^2(V_3 + V_1 + V_2)))r + (K_{m11}S_7^* \\ &+ k_{gsh})h_{max}((K_{m2} + K_{m3})K_{m1} + K_{m2}K_{m3} + d^2)\delta^2)S_2^{*3} + ((-(K_{m11}S_7^* + k_{gsh}) \\ &\times ((K_{m2}K_{m3} + d^2)K_{m1} + (K_{m2} + K_{m3})d^2)\delta h_{max} + ((-V_9K_{m3}K_{m2} + d^2(V_3 - V_9 \\ &+ V_2))K_{m1} + ((V_3 - V_9 + V_1)K_{m2} - K_{m3}(V_9 - V_1 - V_2))d^2)S_7^* + K_{m10}((V_3 + V_2)K_{m1} \\ &+ (V_3 + V_1)K_{m2} + K_{m3}(V_1 + V_2))d^2)r + (K_{m11}S_7^* + k_{gsh})h_{max}((K_{m2}K_{m3} + d^2)K_{m1} \\ &+ (K_{m2} + K_{m3})d^2)\delta^2)S_2^{*2} + d^2((-(K_{m11}S_7^* + k_{gsh})\delta((K_{m2} + K_{m3})K_{m1} \\ &+ K_{m2}K_{m3})h_{max} + (((V_3 - V_9)K_{m2} - K_{m3}(V_9 - V_2))K_{m1} - K_{m2}K_{m3}(V_9 - V_1))S_7^* \\ &+ ((K_{m2}V_3 + K_{m3}V_2)K_{m1} + K_{m2}K_{m3}V_1)K_{m10})r + (K_{m11}S_7^* + k_{gsh})h_{max}\delta^2((K_{m2} \\ &+ K_{m3})K_{m1} + K_{m2}K_{m3}))S_2^* - d^2K_{m3}K_{m2}((\delta(K_{m11}S_7^* + k_{gsh})h_{max} + V_9S_7^*)r \\ &- \delta^2 h_{max}(K_{m11}S_7^* + k_{gsh}))K_{m1}.\end{aligned}$$

For this case, the number of positive roots of (3.3) depends on the signs of $\mathcal{B}_1, \ldots \mathcal{B}_4$. From the positivity condition of S_9^*, we have $r > S_6^*\eta + \delta > \delta$, meaning that $\mathcal{B}_2$ can be positive or negative. Since $\mathcal{B}_1$ and $\mathcal{B}_4$ are positive, then, using Descartes's rule of signs, the number of possible positive roots of (3.3) is given in Table 2. The polynomial (3.3) possibly has at most two positive roots, allowing for multiple positive steady-states in the metabolism system.

Table 2. Number of possible positive roots of S_6^*.

Case	$\mathcal{B}_1$	$\mathcal{B}_2$	$\mathcal{B}_3$	$\mathcal{B}_4$	Number of Sign Changes	Number of Positive Roots
1	+	−	−	+	2	2 or 0
2	+	−	+	+	2	2 or 0
3	+	+	−	+	2	2 or 0
4	+	+	+	+	0	0

Next, from the seventh equation of (2.5), we get the zeros for S_7 in term the roots of polynomial,

$$\mathcal{C}_1 S_7^2 + \mathcal{C}_2 S_7 + \mathcal{C}_3 = 0, \tag{3.4}$$

where

$$\begin{aligned}\mathcal{C}_1 &= -d_g(S_6^* + K_{m11}) < 0,\\ \mathcal{C}_2 &= (-K_{m10}d_g - V_9 + b_g)S_6^* + b_gK_{m11} - d_gk_{gsh},\\ \mathcal{C}_3 &= b_g(K_{m10}S_6^* + k_{gsh}) > 0.\end{aligned}$$

Table 3 shows that the polynomial (3.4) has at most one positive root. In summary, we obtain a possibility for multiple steady-states of systems (2.5). However,

by investigating the steady-state solution using the parameter values in Table 1, we obtain one positive steady-state for the system (2.5) as shown in the first column of Table 4.

Table 3. Number of possible positive roots of S_7^*.

Case	$\mathcal{C}_1$	$\mathcal{C}_2$	$\mathcal{C}_3$	Number of Sign Changes	Number of Positive Roots
1	-	+	+	1	1
2	-	-	+	1	1

Table 4. Steady-state solution (in μM) and eigenvalues of system (2.5).

Steady-state solution	Hurtwitz criteria	Eigenvalue
$S_1^* = 4.12 \times 10^{-29}$	$\omega_1 = 17.4$	$\lambda_1 = -0.24$
$S_2^* = 5.20 \times 10^{-16}$	$\omega_2 = 478.7$	$\lambda_2 = -0.81$
$S_3^* = 6.21 \times 10^{-15}$	$\omega_3 = 2573.9$	$\lambda_3 = -0.29$
$S_4^* = 9.87 \times 10^{-2}$	$\omega_4 = 780.1$	$\lambda_4 = -0.04$
$S_5^* = 2.25 \times 10^{-15}$	$\omega_5 = 4.64$	$\lambda_5 = -15.65$
$S_6^* = 1.70 \times 10^{-17}$		$\lambda_6 = -1.55$
$S_7^* = 8.87 \times 10^{-1}$		$\lambda_7 = -0.08$
$S_8^* = 2.01 \times 10^{-17}$		$\lambda_8 = -0.08$
$S_9^* = 4.06 \times 10^{-26}$		$\lambda_9 = -4$

To investigate the stability of x_E, we linearize the system (2.5) around x_E, which gives us the Jacobian matrix as follows

$$J = \begin{bmatrix} a_{11} & 0 & 0 & 0 & 0 & 0 & 0 & 0 & 0 \\ a_{21} & a_{22} & a_{23} & 0 & 0 & 0 & 0 & 0 & 0 \\ 0 & a_{32} & a_{33} & 0 & 0 & 0 & 0 & 0 & 0 \\ 0 & a_{42} & a_{43} & a_{44} & 0 & 0 & 0 & 0 & 0 \\ 0 & a_{52} & 0 & 0 & a_{55} & 0 & 0 & 0 & 0 \\ 0 & a_{62} & 0 & 0 & 0 & a_{66} & a_{67} & 0 & a_{69} \\ 0 & 0 & 0 & 0 & 0 & a_{76} & a_{77} & 0 & 0 \\ 0 & 0 & 0 & 0 & 0 & a_{86} & a_{87} & a_{88} & 0 \\ 0 & 0 & 0 & 0 & 0 & a_{96} & 0 & 0 & a_{99} \end{bmatrix}, \tag{3.5}$$

where

$$\begin{aligned}
a_{11} &= -k_{al}, \\
a_{21} &= k_{al}, \\
a_{22} &= \left(\frac{V_1}{K_{m1}+S_2^*} - \frac{V_1 S_2^*}{(K_{m1}+S_2^*)^2} + \frac{V_2}{K_{m2}+S_2^*} - \frac{V_2 S_2^*}{(K_{m2}+S_2^*)^2} + \frac{V_3}{K_{m3}+S_2^*} \right. \\
&\quad \left. - \frac{V_3 S_2^*}{(K_{m3}+S_2^*)^2}\right)\left(1+\frac{P(S_2^*)^n}{d^n+(S_2^*)^n}\right) - \left(\frac{V_1 S_2^*}{K_{m1}+S_2^*} + \frac{V_2 S_2^*}{K_{m2}+S_2^*} + \frac{V_3 S_2^*}{K_{m3}+S_2^*}\right) \\
&\quad \left(\frac{P(S_2^*)^n n}{S_2^*(d^n+(S_2^*)^n)} - \frac{P((S_2^*)^n)^2 n}{(d^n+(S_2^*)^n)^2 S_2^*}\right) - \left(\frac{V_4 S_3^*}{K_{m4}S_2^* + K_{m5}S_3^* + S_2^* S_3^* + k_{slt}}\right) \\
&\quad + \left(\frac{V_4 S_2^* S_3^* (K_{m4}+S_3^*)}{(K_{m4}S_2^* + K_{m5}S_3^* + S_2^* S_3^* + k_{slt})^2}\right) - \left(\frac{V_6}{K_{m7}+S_2^*(1+(S_2^*)/K_{i7})}\right) \\
&\quad - \left(\frac{V_5 (S_2^*)^m m}{S_2^*((K_{m6})^m + (S_2^*)^m)}\right) + \left(\frac{V_5((S_2^*)^m)^2 m}{((K_{m6})^m + (S_2^*)^m)^2 S_2^*}\right) \\
&\quad + \left(\frac{V_6 S_2^*(1+(2S_2^*)/K_{i7})}{(K_{m7}+S_2^*(1+(S_2^*)/K_{i7}))^2}\right) - \left(\frac{V_7}{K_{m8}+S_2^*}\right) + \left(\frac{V_7 S_2^*}{(K_{m8}+S_2^*)^2}\right) \\
&\quad - \left(\frac{V_8}{K_{m9}+S_2^*(1+(S_2^*)/K_{i9})}\right) + \left(\frac{V_8 S_2^*(1+(2S_2^*)/K_{i9})}{(K_{m9}+S_2^*(1+(S_2^*)/K_{i9}))^2}\right), \\
a_{23} &= -\left(\frac{V_4 S_2^*}{K_{m4}S_2^* + K_{m5}S_3^* + S_2^* S_3^* + k_{slt}}\right) + \left(\frac{V_4 S_2^* S_3^* (K_{m5}+S_2^*)}{(K_{m4}S_2^* + K_{m5}S_3^* + S_2^* S_3^* + k_{slt})^2}\right), \\
a_{32} &= -\left(\frac{V_4 S_3^*}{K_{m4}S_2^* + K_{m5}S_3^* + S_2^* S_3^* + k_{slt}}\right) + \left(\frac{V_4 S_2^* S_3^* (K_{m4}+S_3^*)}{(K_{m4}S_2^* + K_{m5}S_3^* + S_2^* S_3^* + k_{slt})^2}\right), \\
a_{33} &= -\left(\frac{V_4 S_2^*}{K_{m4}S_2^* + K_{m5}S_3^* + S_2^* S_3^* + k_{slt}}\right) + \left(\frac{V_4 S_2^* S_3^* (K_{m5}+S_2^*)}{(K_{m4}S_2^* + K_{m5}S_3^* + S_2^* S_3^* + k_{slt})^2}\right) - d_s, \\
a_{42} &= -\left(\frac{V_4 S_3^*}{K_{m4}S_2^* + K_{m5}S_3^* + S_2^* S_3^* + k_{slt}}\right) + \left(\frac{V_4 S_2^* S_3^* (K_{m4}+S_3^*)}{(K_{m4}S_2^* + K_{m5}S_3^* + S_2^* S_3^* + k_{slt})^2}\right), \\
a_{43} &= -\left(\frac{V_4 S_2^*}{K_{m4}S_2^* + K_{m5}S_3^* + S_2^* S_3^* + k_{slt}}\right) + \left(\frac{V_4 S_2^* S_3^* (K_{m5}+S_2^*)}{(K_{m4}S_2^* + K_{m5}S_3^* + S_2^* S_3^* + k_{slt})^2}\right), \\
a_{44} &= -k_{sl},
\end{aligned}$$

$$
\begin{aligned}
a_{52} &= -\left(\frac{V_5(S_2^*)^m m}{S_2^*((K_{m6})^m + (S_2^*)^m)}\right) + \left(\frac{V_5((S_2^*)^m)^2 m}{((K_{m6})^m + (S_2^*)^m)^2 S_2^*}\right) + \left(\frac{V_7 S_2^*}{(K_{m8} + S_2^*)^2}\right) \\
&\quad + \left(\frac{V_6 S_2^*(1 + (2S_2^*)/K_{i7})}{(K_{m7} + S_2^*(1 + (S_2^*)/K_{i7}))^2}\right) - \left(\frac{V_7}{K_{m8} + S_2^*}\right) - \left(\frac{V_6}{K_{m7} + S_2^*(1 + (S_2^*)/K_{i7})}\right) \\
&\quad - \left(\frac{V_8}{K_{m9} + S_2^*(1 + (S_2^*)/K_{i9})}\right) + \left(\frac{V_8 S_2^*(1 + (2S_2^*)/K_{i9})}{(K_{m9} + S_2^*(1 + (S_2^*)/K_{i9}))^2}\right), \\
a_{55} &= -k_{gl}, \\
a_{66} &= -\frac{V_9 S_7^*}{K_{m10}S_6^* + K_{m11}S_7^* + S_6^*S_7^* + k_{gsh}} + \frac{V_9 S_6^* S_7^*(K_{m10} + S_7^*)}{(K_{m10}S_6^* + K_{m11}S_7^* + S_6^*S_7^* + k_{gsh})^2} - \eta S_9^*, \\
a_{67} &= -\frac{V_9 S_6^*}{K_{m10}S_6^* + K_{m11}S_7^* + S_6^*S_7^* + k_{gsh}} + \frac{V_9 S_6^* S_7^*(K_{m11} + S_6^*)}{(K_{m10}S_6^* + K_{m11}S_7^* + S_6^*S_7^* + k_{gsh})^2}, \\
a_{69} &= -\eta S_6^*, \\
a_{76} &= -\frac{V_9 S_7^*}{K_{m10}S_6^* + K_{m11}S_7^* + S_6^*S_7^* + k_{gsh}} + \frac{V_9 S_6^* S_7^*(K_{m10} + S_7^*)}{(K_{m10}S_6^* + K_{m11}S_7^* + S_6^*S_7^* + k_{gsh})^2}, \\
a_{77} &= -\frac{V_9 S_6^*}{K_{m10}S_6^* + K_{m11}S_7^* + S_6^*S_7^* + k_{gsh}} + \frac{V_9 S_6^* S_7^*(K_{m11} + S_6^*)}{(K_{m10}S_6^* + K_{m11}S_7^* + S_6^*S_7^* + k_{gsh})^2}, \\
a_{86} &= -\frac{V_9 S_7^*}{K_{m10}S_6^* + K_{m11}S_7^* + S_6^*S_7^* + k_{gsh}} + \frac{V_9 S_6^* S_7^*(K_{m10} + S_7^*)}{(K_{m10}S_6^* + K_{m11}S_7^* + S_6^*S_7^* + k_{gsh})^2}, \\
a_{87} &= -\frac{V_9 S_6^*}{K_{m10}S_6^* + K_{m11}S_7^* + S_6^*S_7^* + k_{gsh}} + \frac{V_9 S_6^* S_7^*(K_{m11} + S_6^*)}{(K_{m10}S_6^* + K_{m11}S_7^* + S_6^*S_7^* + k_{gsh})^2}, \\
a_{88} &= -k_{nqgl}, \\
a_{96} &= -\eta S_9^*, \\
a_{99} &= r\left(1 - \frac{S_9^*}{h_{\max}}\right) - \frac{rS_9^*}{h_{\max}} - \eta S_6^* - \delta.
\end{aligned}
$$

It is easy to show that the eigenvalues of J are $\lambda_1 = a_{11} = -k_{al}$, $\lambda_2 = a_{44} = -k_{sl}$, $\lambda_3 = a_{55} = -k_{gl}$, and $\lambda_4 = a_{88} = -k_{nqgl}$. The other eigenvalues are obtained by solving the polynomial

$$\lambda^5 + c_1\lambda^4 + c_2\lambda^3 + c_3\lambda^2 + c_4\lambda + c_5 = 0, \tag{3.6}$$

where

$$
\begin{aligned}
c_1 &= -(a_{99} + a_{77} + a_{66} + a_{33} + a_{22}), \\
c_2 &= -(-a_{22}a_{33} - a_{22}a_{66} - a_{22}a_{77} - a_{22}a_{99} + a_{23}a_{32} - a_{33}a_{66} - a_{33}a_{77} - a_{33}a_{99} \\
&\quad - a_{66}a_{77} - a_{66}a_{99} + a_{67}a_{76} + a_{69}a_{96} - a_{77}a_{99}), \\
c_3 &= -(a_{22}a_{33}a_{66} + a_{22}a_{33}a_{77} + a_{22}a_{33}a_{99} + a_{22}a_{66}a_{77} + a_{22}a_{66}a_{99} - a_{22}a_{67}a_{76} \\
&\quad - a_{22}a_{69}a_{96} + a_{22}a_{77}a_{99} - a_{23}a_{32}a_{66} - a_{23}a_{32}a_{77} - a_{23}a_{32}a_{99} + a_{33}a_{66}a_{77} \\
&\quad + a_{33}a_{66}a_{99} - a_{33}a_{67}a_{76} - a_{33}a_{69}a_{96} + a_{33}a_{77}a_{99} + a_{66}a_{77}a_{99} - a_{67}a_{76}a_{99} \\
&\quad - a_{69}a_{77}a_{96}), \\
c_4 &= -(-a_{22}a_{33}a_{66}a_{77} - a_{22}a_{33}a_{66}a_{99} + a_{22}a_{33}a_{67}a_{76} + a_{22}a_{33}a_{69}a_{96} \\
&\quad - a_{22}a_{33}a_{77}a_{99} - a_{22}a_{66}a_{77}a_{99} + a_{22}a_{67}a_{76}a_{99} + a_{22}a_{69}a_{77}a_{96} + a_{23}a_{32}a_{66}a_{77} \\
&\quad + a_{23}a_{32}a_{66}a_{99} - a_{23}a_{32}a_{67}a_{76} - a_{23}a_{32}a_{69}a_{96} + a_{23}a_{32}a_{77}a_{99} - a_{33}a_{66}a_{77}a_{99} \\
&\quad + a_{33}a_{67}a_{76}a_{99} + a_{33}a_{69}a_{77}a_{96}), \\
c_5 &= -a_{22}a_{33}a_{66}a_{77}a_{99} + a_{22}a_{33}a_{67}a_{76}a_{99} + a_{22}a_{33}a_{69}a_{77}a_{96} + a_{23}a_{32}a_{66}a_{77}a_{99} \\
&\quad - a_{23}a_{32}a_{67}a_{76}a_{99} - a_{23}a_{32}a_{69}a_{77}a_{96}.
\end{aligned}
$$

Routh-Hurwitz criterion [23] gives the conditions for (3.6) to have roots with negative real parts. The conditions are $\omega_1 = c_1 > 0$; $\omega_2 = c_1c_2 - c_3 > 0$; $\omega_3 = c_1c_2c_3 - c_3^2 + c_1^2c_4 > 0$; $\omega_4 = c_1c_2c_3c_4 - c_1^2c_4^2 + c_3^2c_4 > 0$; $\omega_5 = c_1c_2c_3c_4c_5 + 2c_1c_4c_5^2 + c_2c_3c_5^2 - c_1^2c_4^2c_5 + c_1c_2^2c_5^2 + c_3^2c_4c_5 + c_5^3 > 0$. By using parameter values in Table 1, the stability conditions given by the Routh-Hurwitz criterion are fulfilled, and we obtain the eigenvalues of J as shown in the second and the third columns of Table 4, which guarantee the local stability of x_E.

3.2. Sensitivity analysis of acetaminophen metabolism

For this part, we perform sensitivity analysis of the reactions within the metabolic pathway using Metabolic Control Analysis (MCA). MCA is a quantitative method used to assess the impacts of disturbances in metabolic networks [25]. MCA also evaluates the significant role of each enzyme in regulating flux. Reaction sensitivity is determined through elasticity coefficients and control coefficients for steady-state reaction rate and metabolites [26]. The sensitivity of the reaction rate $\mathbf{p}$ to the changes of metabolite $\mathbf{S}$ is quantified by the elasticity coefficient, defined as

$$\varepsilon_{\mathbf{S}}^{\mathbf{p}} = \left(\frac{\mathbf{S}}{\mathbf{p}}\right)\left(\frac{\partial \mathbf{p}}{\partial \mathbf{S}}\right). \tag{3.7}$$

Similarly, for the metabolite concentration $\mathbf{S}$, it is represented by the control coefficient

$$C_{\mathbf{p}}^{\mathbf{S}} = \left(\frac{\mathbf{p}}{\mathbf{S}}\right)\left(\frac{\partial \mathbf{S}}{\partial \mathbf{p}}\right). \tag{3.8}$$

These control coefficients can be determined using matrix control techniques involving the system's stoichiometric matrix (2.5). Considering the kinetic model in the system (2.5), it can be reformulated as follows

$$\frac{d\mathbf{S}}{dt} = N\mathbf{p}(\mathbf{S}, \mathbf{x}). \tag{3.9}$$

Here, $\mathbf{S} = (S_2, \ldots, S_8)$ represents the vector of metabolite concentrations, and $\mathbf{p} = (p_1, \ldots, p_{13})$ represents the vector of reaction rates [27]. The kinetic equation p_k is defined in (2.1-2.4). The reaction rates $\mathbf{p}$ are dependent on both the metabolite concentrations $\mathbf{S}$ and the kinetic parameters $\mathbf{x}$, which are listed in Table 1.

Figure 1 shows that 13 reactions convert seven substances. This gives a stoichiometric matrix N of dimension 7×13. In a stoichiometric matrix, the number of rows reflects the number of substrates involved, while the number of columns reflects the number of chemical reactions [28]. By augmenting the matrix N with an identity matrix, we obtain the augmented matrix $[N|I]$ as follows

$$\left(\begin{array}{cccccccccccc|ccccccc}
-1 & -1 & -1 & 0 & 1 & 0 & 0 & 0 & 0 & 0 & 0 & 0 & 0 & 1 & 0 & 0 & 0 & 0 & 0 & 0 \\
0 & -1 & 0 & 0 & 0 & -1 & 0 & 0 & 0 & 0 & 0 & 0 & 0 & 0 & 1 & 0 & 0 & 0 & 0 & 0 \\
0 & 1 & 0 & 0 & 0 & 0 & -1 & 1 & 0 & 0 & 0 & 0 & 0 & 0 & 0 & 1 & 0 & 0 & 0 & 0 \\
0 & 0 & 1 & 0 & 0 & 0 & 0 & 0 & -1 & 0 & 0 & 0 & 0 & 0 & 0 & 0 & 1 & 0 & 0 & 0 \\
1 & 0 & 0 & -1 & 0 & 0 & 0 & 0 & 0 & -1 & 0 & 0 & 0 & 0 & 0 & 0 & 0 & 1 & 0 & 0 \\
0 & 0 & 0 & -1 & 0 & 0 & 0 & 0 & 0 & 0 & 1 & -1 & 0 & 0 & 0 & 0 & 0 & 0 & 1 & 0 \\
0 & 0 & 0 & 1 & 0 & 0 & 0 & 0 & 0 & 0 & 0 & 0 & -1 & 0 & 0 & 0 & 0 & 0 & 0 & 1
\end{array}\right).$$

After applying Gaussian elimination, the augmented matrix $[N|I]$ is transformed into its reduced row echelon form, given as

$$\left(\begin{array}{ccccccccccc|ccccccc} 1&0&0&0&0&0&0&0&0&-1&0&0&-1&0&0&0&1&0&1\\ 0&1&0&0&0&0&1&-1&0&0&0&0&0&0&1&0&0&0&0\\ 0&0&1&0&0&0&0&0&-1&0&0&0&0&0&0&1&0&0&0\\ 0&0&0&1&0&0&0&0&0&0&0&0&-1&0&0&1&0&0&1\\ 0&0&0&0&1&0&1&1&-1&-1&0&0&-1&1&0&1&1&0&1\\ 0&0&0&0&0&1&-1&1&0&0&0&0&0&0&-1&-1&0&0&0\\ 0&0&0&0&0&0&0&0&0&0&1&-1&-1&0&0&0&0&1&1 \end{array}\right).$$

The result of the elimination indicates that the rows of N are linearly independent, confirming that the rank of the matrix N is 7. Since the rank of N equals to the number of metabolites (7), no further reduction is required. When $N\mathbf{p}(S,x)=\mathbf{0}$, a steady-state reaction rate vector, denoted as the flux vector J, is achieved. Given that the rank of N is 7, there are 6 column vectors (denoted as $J_1,\ldots,J_6$) that form a basis for the null space of N. If we define matrix K with columns $J_1,\ldots,J_6$, then $NK=N[J_1|\ldots|J_6]=[NJ_1|\ldots|NJ_6]=\mathbf{0}$.

For any 13-dimensional flux column vector J, it can be expressed as $J=KJ_{\mathrm{id}}$, where J_{id} is a 6-dimensional column vector of independent fluxes. In this case, J_{id} is not unique. Here, we choose $J_{\mathrm{id}}=(J_1,J_4,J_8,J_9,J_{10},J_{11})$ representing the independent fluxes. So, from the relation of J_i and J_{id}, we have

$$K=\begin{bmatrix} 1&0&0&0&0&0\\ 0&0&0&1&0&1\\ 1&-1&0&0&0&0\\ 0&1&0&0&0&0\\ 0&0&1&0&0&0\\ 0&0&0&0&0&1\\ 1&-1&1&1&0&1\\ 0&0&1&0&0&0\\ 0&0&0&1&0&0\\ 0&0&0&0&1&0\\ 0&0&0&0&0&1\\ 1&0&0&0&0&0\\ 0&0&0&0&1&1 \end{bmatrix}. \tag{3.10}$$

Two theorems can be used to determine the control matrices for fluxes and metabolites in a system. These theorems are the summation theorem and the connectivity theorem [29]. The normalized forms of these theorems are written as follows:

$$\begin{pmatrix} C_J & C_S \end{pmatrix}\begin{pmatrix} \mathcal{K} \\ -M_\varepsilon \end{pmatrix}=\begin{pmatrix} \mathcal{K} & 0 \\ 0 & I \end{pmatrix}, \tag{3.11}$$

where C_J and C_S represent the normalized control matrices for fluxes and metabolites, respectively [30]. Matrix $\mathcal{K}$ is the normalized form of the kernel of the matrix N, I is the identity matrix, and M_ε is the elasticity matrix. Next, the control matrices for fluxes (C_J) and metabolites (C_S) is determined, which can be written as:

$$\begin{pmatrix} C_J & C_S \end{pmatrix} = \begin{pmatrix} \mathcal{K} & 0 \\ 0 & I \end{pmatrix} \begin{pmatrix} \mathcal{K} & -M_\varepsilon \end{pmatrix}^{-1}. \tag{3.12}$$

Matrix K represents the dependency of reaction rates in steady-state conditions (fluxes) on the independent fluxes. The matrix K can be normalized using the equation $\mathcal{K} = D_J^{-1} K D_{J_i}$, where D_J is the diagonal matrix of fluxes. The normalization process allows us to obtain the following:

$$\mathcal{K} = \begin{bmatrix} 1 & 0 & 0 & 0 & 0 & 0 \\ 0 & 0 & 0 & \frac{j_9}{j_2} & 0 & \frac{j_{11}}{j_2} \\ \frac{j_1}{j_3} & -\frac{j_4}{j_3} & 0 & 0 & 0 & 0 \\ 0 & 1 & 0 & 0 & 0 & 0 \\ 0 & 0 & \frac{j_8}{j_5} & 0 & 0 & 0 \\ 0 & 0 & 0 & 0 & 0 & \frac{j_{11}}{j_6} \\ \frac{j_1}{j_7} & -\frac{j_4}{j_7} & \frac{j_8}{j_7} & \frac{j_9}{j_7} & 0 & \frac{j_{11}}{j_7} \\ 0 & 0 & 1 & 0 & 0 & 0 \\ 0 & 0 & 0 & 1 & 0 & 0 \\ 0 & 0 & 0 & 0 & 1 & 0 \\ 0 & 0 & 0 & 0 & 0 & 1 \\ \frac{j_1}{j_{12}} & 0 & 0 & 0 & 0 & 0 \\ 0 & 0 & 0 & 0 & \frac{j_{10}}{j_{13}} & \frac{j_{11}}{j_{13}} \end{bmatrix}. \tag{3.13}$$

In metabolic control analysis, the elasticity coefficient measures the sensitivity of a reaction rate to changes in concentration or parameters. It quantifies the direct effect on reaction rates while keeping other aspects of the network unchanged. The sensitivity of the reaction rate p_k of a reaction to changes in concentration S_i of a metabolite is calculated using the elasticity coefficient:

$$\varepsilon_i^k = \frac{S_i}{p_k} \left(\frac{\partial p_k}{\partial S_i} \right). \tag{3.14}$$

This coefficient is commonly referred to as the elasticity matrix. This matrix contains the elasticity coefficients of each reaction rate for every metabolite, as shown in the following matrix:

$$M_\varepsilon = \begin{bmatrix} \varepsilon_{S_2}^{p_1} & 0 & 0\,0 & 0 & 0 & 0 \\ \varepsilon_{S_2}^{p_2} & \varepsilon_{S_3}^{p_2} & 0\,0 & 0 & 0 & 0 \\ \varepsilon_{S_2}^{p_3} & 0 & 0\,0 & 0 & 0 & 0 \\ 0 & 0 & 0\,0 & \varepsilon_{S_6}^{p_4} & \varepsilon_{S_7}^{p_4} & 0 \\ 0 & 0 & 0\,0 & 0 & 0 & 0 \\ 0 & 1 & 0\,0 & 0 & 0 & 0 \\ 0 & 0 & 0\,0 & 0 & 0 & 0 \\ 0 & 0 & 1\,0 & 0 & 0 & 0 \\ 0 & 0 & 0\,1 & 0 & 0 & 0 \\ 0 & 0 & 0\,0 & 1 & 0 & 0 \\ 0 & 0 & 0\,0 & 0 & 1 & 0 \\ 0 & 0 & 0\,0 & 0 & 0 & 0 \\ 0 & 0 & 0\,0 & 0 & 0 & 1 \end{bmatrix}, \tag{3.15}$$

with

$$\varepsilon_{S_2}^{p_1} = \frac{1}{\left(\frac{V_1}{K_{m1}+S_2^*} + \frac{V_2}{K_{m2}+S_2^*} + \frac{V_3}{K_{m3}+S_2^*}\right)\left(1+\frac{P(S_2^*)^n}{d^n+(S_2^*)^n}\right)} \left(S_2^* \left(\frac{V_1}{K_{m1}+S_2^*} - \frac{V_1 S_2^*}{(K_{m1}+S_2^*)^2} \right) + \left(\frac{V_2}{K_{m2}+S_2^*} - \frac{V_2 S_2^*}{(K_{m2}+S_2^*)^2} \right) + \left(\frac{V_3}{K_{m3}+S_2^*} - \frac{V_3 S_2^*}{(K_{m3}+S_2^*)^2} \right) \left((1+\frac{P(S_2^*)^n}{d^n+(S_2^*)^n} \right) + \left(\frac{V_1 S_2^*}{K_{m1}+S_2^*} + \frac{V_2 S_2^*}{K_{m2}+S_2^*} + \frac{V_3 S_2^*}{K_{m3}+S_2^*} \right) \left(\frac{P(S_2^*)^n n}{S_2^*(d^n+(S_2^*)^n)} - \frac{P((S_2^*)^n)^2 n}{(d^n+(S_2^*)^n)^2 S_2^*} \right) \right),$$

$$\varepsilon_{S_2}^{p_2} = \left(\frac{V_4 S_3^*}{K_{m4}S_2^* + K_{m5}S_3^* + S_2^*S_3^* + k_{slt}} - \frac{V_4 S_2^* S_3^* (K_{m4}+S_3^*)}{(K_{m4}S_2^* + K_{m5}S_3^* + S_2^*S_3^* + k_{slt})^2} \right) \frac{K_{m4}S_2^* + K_{m5}S_3^* + S_2^*S_3^* + k_{slt}}{V_4 S_3^*},$$

$$\varepsilon_{S_3}^{p_2} = \left(\frac{V_4 S_2^*}{K_{m4}S_2^* + K_{m5}S_3^* + S_2^*S_3^* + k_{slt}} - \frac{V_4 S_2^* S_3^* (K_{m5}+S_2^*)}{(K_{m4}S_2^* + K_{m5}S_3^* + S_2^*S_3^* + k_{slt})^2} \right) \frac{K_{m4}S_2^* + K_{m5}S_3^* + S_2^*S_3^* + k_{slt}}{V_4 S_2^*},$$

$$\varepsilon_{S_2}^{p_3} = \frac{1}{\left(\frac{V_5(S_2)^n}{(K_{m6})^n+(S_2)^n} + \frac{V_6 S_2}{K_{m7}+S_2(1+S_2/K_{i7})} + \frac{V_7 S_2}{K_{m8}+S_2} + \frac{V_8 S_2}{K_{m9}+S_2(1+S_2/K_{i9})}\right)} \left(-S_2^* \left(-\left(\frac{V_5 (S_2^*)^m m}{S_2^*((K_{m6})^m + (S_2^*)^m)} \right) \right) + \left(\frac{V_5((S_2^*)^m)^2 m}{((K_{m6})^m + (S_2^*)^m)^2 S_2^*} \right) - \left(\frac{V_6}{K_{m7}+S_2^*(1+S_2^*/K_{i7})} \right) + \left(\frac{V_6 S_2^*(1+2S_2^*/K_{i7})}{(K_{m7}+S_2^*(1+S_2^*/K_{i7}))^2} \right) - \left(\frac{V_7}{K_{m8}+S_2^*} \right) + \left(\frac{V_8 S_2^*(1+2S_2^*/K_{i9})}{(K_{m9}+S_2^*(1+S_2^*/K_{i9}))^2} \right) - \left(\frac{V_8}{K_{m9}+S_2^*(1+S_2^*/K_{i9})} \right) + \left(\frac{V_7 S_2^*}{(K_{m8}+S_2^*)^2} \right) \right),$$

$$\varepsilon_{S_6}^{p_4} = \left(\frac{V_9 S_7^*}{K_{m10} S_6^* + K_{m11} S_7^* + S_6^* S_7^* + k_{gsh}} - \frac{V_9 S_6^* S_7^* (K_{m10} + S_7^*)}{(K_{m10} S_6^* + K_{m11} S_7^* + S_6^* S_7^* + k_{gsh})^2} \right) \frac{K_{m10} S_6^* + K_{m11} S_7^* + S_6^* S_7^* + k_{gsh}}{V_9 S_7^*},$$

$$\varepsilon_{S_7}^{p_4} = \left(\frac{V_9 S_6^*}{K_{m10} S_6^* + K_{m11} S_7^* + S_6^* S_7^* + k_{gsh}} - \frac{V_9 S_6^* S_7^* (K_{m11} + S_6^*)}{(K_{m10} S_6^* + K_{m11} S_7^* + S_6^* S_7^* + k_{gsh})^2} \right) \frac{K_{m10} S_6^* + K_{m11} S_7^* + S_6^* S_7^* + k_{gsh}}{V_9 S_6^*}.$$

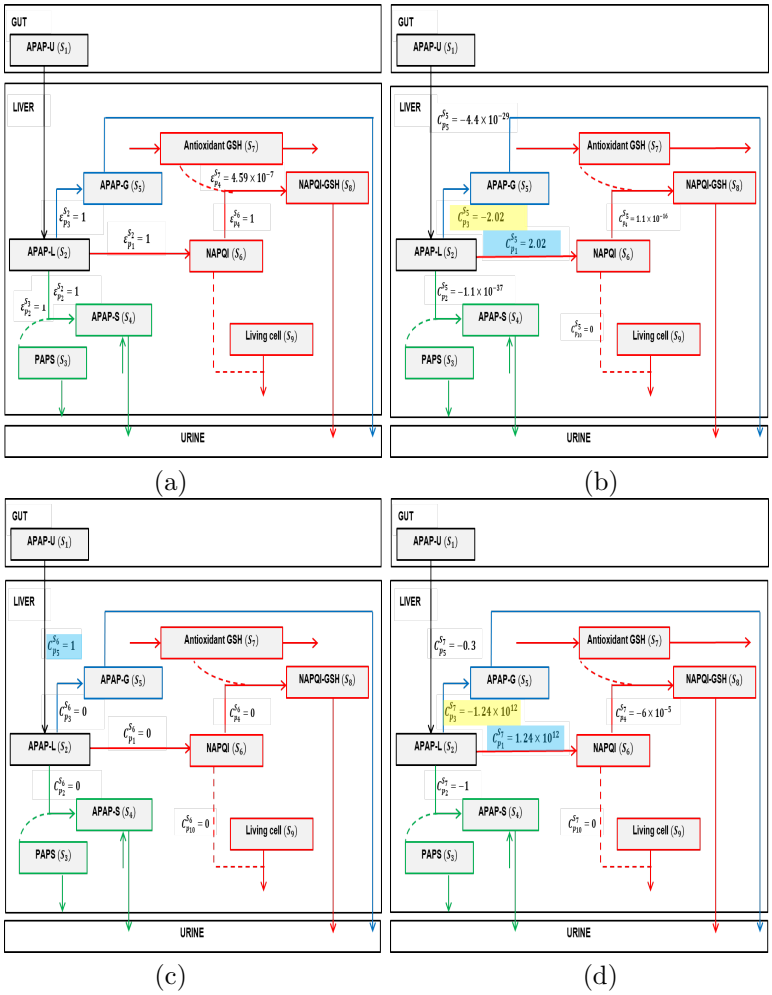

Figure 2. Distribution of: (a) elasticity coefficients that measure the local effect of reaction changes; (b) control coefficients that measure the global effect of reaction changes on the changes in APAP-G concentration (S_5); (c) NAPQI concentration (S_6); and (d) GSH antioxidant concentration (S_7). The sensitivity analysis only focuses on the input rate of APAP from the gut and reactions catalyzed by enzymes. The highest positive control is shaded with blue, and the highest negative control is shaded with yellow.

Using the kinetic parameters in Table 1 and the steady-state solution in Table 4, we obtain the sensitivity results that are distributed in Figure 2. Figure 2-(a) shows the distribution of elasticity coefficients, which indicates the sensitivity of reaction

rates to the changes in metabolite concentrations. Since the elasticity coefficient quantifies the response of the local reaction p_k to the changes in metabolite concentration S, it only reflects a local property, specifically the property of the reaction rate p. For instance, for the first reaction, we have $\varepsilon_{p_1}^{S_1} = 1$, indicating that when the concentration of S_1 is increased, then the reaction rate p_1 also increases by the same magnitude.

Furthermore, the obtained control coefficients are essential for quantifying the global impact of changes in enzyme activity on metabolite concentrations. The coefficients $C_{p_k}^{S_5}$, $C_{p_k}^{S_6}$, and $C_{p_k}^{S_7}$ represent the sensitivity of the APAP-G, NAPQI, and GSH concentrations based on the reaction rate p_k, respectively. A positive control coefficient indicates that increasing the reaction rate affects the increase in the steady-state concentration of APAP-G, NAPQI, and GSH. In contrast, a negative coefficient suggests the opposite effect. Distribution of global sensitivity effects of reactions to the changes of APAP-G, NAPQI, and the antioxidant glutathione GSH is measured by control coefficients, as shown in Figure 2-(b,c,d). For NAPQI, the highest sensitive reaction with positive control for increasing its concentration is regulated by APAP reaction (p_5). This reaction represents the input rate of acetaminophen from the gut to the liver. The highest input rate of acetaminophen from the gut is the highest NAPQI concentration that will be produced. There are no controls from the other reactions indicated by the zero control coefficient results (see 2-(c)). Therefore, the concentration of NAPQI is solely determined by the number of consumed drug dosages. On the other hand, the increase of APAP-G and GSH concentrations is highly regulated by CYP reaction (p_1) with the highest positive control and UGT reaction (p_3) with the highest negative control. For the other enzymatic reactions, the global effects concerning the APAP-G and GSH changes are different, as shown by their control values (see Figure 2-(d)). For instance, increasing 1% of the maximum reaction rate of CYP leads to the increase of GSH concentration with magnitude $C_{p_1}^{S_7}$ (blue shading on Figure 2-(d)), while increasing 1% of the maximum rate of UGT will decrease the concentration of GSH with the magnitude of $C_{p_3}^{S_7}$.

4. Optimal control of acetaminophen metabolism

One of the pharmacological strategies to prevent hepatotoxicity is to increase the concentration of the antioxidant GSH because it can help detoxify toxic metabolites (NAPQI) by conjugating them with GSH, which are ultimately excreted. The sensitivity analysis results indicate that p_3, catalyzed by uridine 5'-diphosphate-glucuronosyltransferase (UGT), is the reaction rate with the highest negative effect on antioxidant GSH concentration, while p_1, catalyzed by cytochrome (CYP), is the reaction rate with the highest positive effect. It means that controlling the maximum activity of the UGT and the CYP is the key regulation for reducing hepatotoxicity. We then define a regulation rule as follows:

$$p_k^*(S; u_i) = p_k(S; V_{\max}(1 - u_i)), k = 1, 3, i = 1, 2, \tag{4.1}$$

where u_1 and u_2 are the percentage of changes of the maximum activity ($V_{\max}$) of UGT and CYP, respectively. Equation (4.1) indicates that the optimized reaction rate p_k^* depends on the original reaction rate p, adjusted by the factor $V_{\max}(1-u_i)$. To minimize the activity of CYP and maximize the activity of UGT together with

maximizing the concentration of GSH, we define the following objective function J:

$$\min_{(u_1,u_2)} J(u_1,u_2) = \min_{(u_1,u_2)} \int_{t_0}^{t_f} (-\xi_1 S_7 + \xi_2 u_1^2 - \xi_3 u_2^2)\, dt, \tag{4.2}$$

subject to the system in (2.5). Variables ξ_1, ξ_2, and ξ_3 are weighting factors of the respective objectives, S_7 is the concentration of the antioxidant GSH, p_1 is the reaction rate catalyzed by CYP, and p_3 is the reaction rate catalyzed by UGT. Based on the Pontryagin minimum principle [31], the first step in solving the objective function (4.2) with constraint (2.5) is to determine the Hamiltonian function. The Hamiltonian for this problem can be written as

$$H(t, \mathbf{S}, \mathbf{u}, \boldsymbol{\lambda}) = (-\xi_1 S_7 + \xi_2 u_1^2 - \xi_3 u_2^2) + \boldsymbol{\lambda}^T(t) g(t, \mathbf{S}, \mathbf{u}), \tag{4.3}$$

where $g(t, \mathbf{S}, \mathbf{u})$ is the right hand side of system (2.5). The costate variable is given as

$$\boldsymbol{\lambda} = (\lambda_1, \lambda_2, \lambda_3, \lambda_4, \lambda_5, \lambda_6, \lambda_7, \lambda_8, \lambda_9)^T. \tag{4.4}$$

For the state equation $\mathbf{S}$, we obtain

$$\dot{\boldsymbol{S}} = \frac{\partial H}{\partial \boldsymbol{\lambda}} = \left(\frac{\partial H}{\partial \lambda_1}, \frac{\partial H}{\partial \lambda_2}, \frac{\partial H}{\partial \lambda_3}, \frac{\partial H}{\partial \lambda_4}, \frac{\partial H}{\partial \lambda_5}, \frac{\partial H}{\partial \lambda_6}, \frac{\partial H}{\partial \lambda_7}, \frac{\partial H}{\partial \lambda_8}, \frac{\partial H}{\partial \lambda_9} \right)^T. \tag{4.5}$$

For the costate equation, we obtain

$$\dot{\boldsymbol{\lambda}} = -\frac{\partial H}{\partial \mathbf{S}} = \left(-\frac{\partial H}{\partial S_1}, -\frac{\partial H}{\partial S_2}, -\frac{\partial H}{\partial S_3}, -\frac{\partial H}{\partial S_4}, -\frac{\partial H}{\partial S_5}, -\frac{\partial H}{\partial S_6}, -\frac{\partial H}{\partial S_7}, -\frac{\partial H}{\partial S_8}, -\frac{\partial H}{\partial S_9} \right). \tag{4.6}$$

Furthermore, for the stationary condition, we have

$$\frac{\partial H}{\partial \mathbf{u}} = \left(\frac{\partial H}{\partial u_1}, \frac{\partial H}{\partial u_2} \right)^T = \mathbf{0}. \tag{4.7}$$

By solving Equation (4.7), we obtain

$$u_1 = \frac{(S_2^n P + S_2^n + d^n) S_2 V_2 (\lambda_2 - \lambda_6)}{(d^n + S_2^n)(K_{m2} + S_2)\xi_2}, \tag{4.8}$$

$$u_2 = -\frac{K_{i9} S_2 V_8 (\lambda_2 + \lambda_5)}{((S_2 + K_{m9}) K_{i9} + S_2^2)\xi_3}. \tag{4.9}$$

Based on the boundary conditions for u_1 and u_2, $0 \le u_1 \le 1$ and $0 \le u_2 \le 1$, the optimal control for u_1^* and u_2^* are determined as follows

$$u_1^* = \begin{cases} u_1, & \text{if } 0 \le u_1 \le 1, \\ 0, & \text{if } u_1 < 0, \\ 1, & \text{if } u_1 > 1, \end{cases} \tag{4.10}$$

or

$$u_1^* = \min\{1, \max\{0, u_1\}\}, \tag{4.11}$$

with u_1 as described in Equation (4.8), and

$$u_2^* = \begin{cases} u_2, & \text{if } 0 \leq u_2 \leq 1, \\ 0, & \text{if } u_2 < 0, \\ 1, & \text{if } u_2 > 1, \end{cases} \tag{4.12}$$

or

$$u_2^* = \min\{1, \max\{0, u_2\}\}, \tag{4.13}$$

with u_2 as described in Equation (4.9). Therefore, we obtain the optimal control for the percentage regulation of CYP and UGT as shown in (4.11) and (4.13). In the next section, we will present numerical simulations to capture the system's dynamics and to explore the effects of the sensitivity of CYP and UGT and the application of the optimal control obtained.

5. Numerical simulation

This section presents simulations of the acetaminophen metabolism model without control and with control applied to the chosen reaction rates. The regulated reactions are selected based on the sensitivity results obtained in the previous analysis. The simulation is carried out by using parameter values given in Table 1 and initial condition for APAP in the gut (APAP-U), $S_1(0)= 7\mu M$. This APAP concentration represents an overdose condition [9]. The other metabolites have initial conditions: $S_2(0) = 4\ \mu M$, $S_3(0) = 1\ \mu M$, $S_4(0) = 1\ \mu M$, $S_5(0) = 0\ \mu M$, $S_6(0) = 0\ \mu M$, $S_7(0) = 0.5\ \mu M$, $S_8(0) = 0\ \mu M$, and $S_9(0) = 0.2\ \mu M$. The first simulation is presented for various levels of the maximum rate of CYP. The CYP consists of three cytochrome oxidases, i.e., CYP1A2, CYP2E1, and CYP3A4. Among the three cytochrome oxidases, CYP2E1 is the reaction that highly affects the CYP [41]. If we manually increase the maximum rate of CYP3A4 (V_2) on p_1, we get the regulatory effects on the entire metabolite on the liver pathway as shown in Figure 3. Among all the metabolites, the regulation of CYP significantly affects the concentration of APAP-L in the liver, NAPQI, GSH, and the complex of NAPQI-GSH (see Figure 3-(b,f,g,h)). Increasing the reaction rate p_1 also increases the concentration of NAPQI and NAPQI-GSH complex and, consequently, decreases the concentration of APAP-L and GSH due to CYP converting APAP-L on the liver into NAPQI as the toxic compound. Increasing the NAPQI concentration affects the increase of the complex NAPQI-GSH, which also decreases the concentration of GSH. For instance, when we increase the reaction rate of CYP by 29%, the concentration of NAPQI will also increase by almost one hundred percent. On the contrary, increasing the rate of CYP by 29% decreases the concentration of GSH by one hundred percent. For acetaminophen glucuronide (APAP-G) that will be excreted in the urine, the concentration decreases by five percent. For other metabolites, the regulation carried out did not provide significant effects (see Figure 3-(a,c,d,i)).

In the following simulation, we present the optimal control results that were obtained by regulating two reactions that have the highest positive and the highest negative control to the changes of GSH concentration, i.e., the maximum reaction rate of CYP (p_1) and UGT (p_3). The optimization task is to find the best percentage of CYP's maximum reaction rate changes (u_1) and UGT (u_2). The best regulation of CYP and UGT is expected to maximize the production rate of GSH, such that the

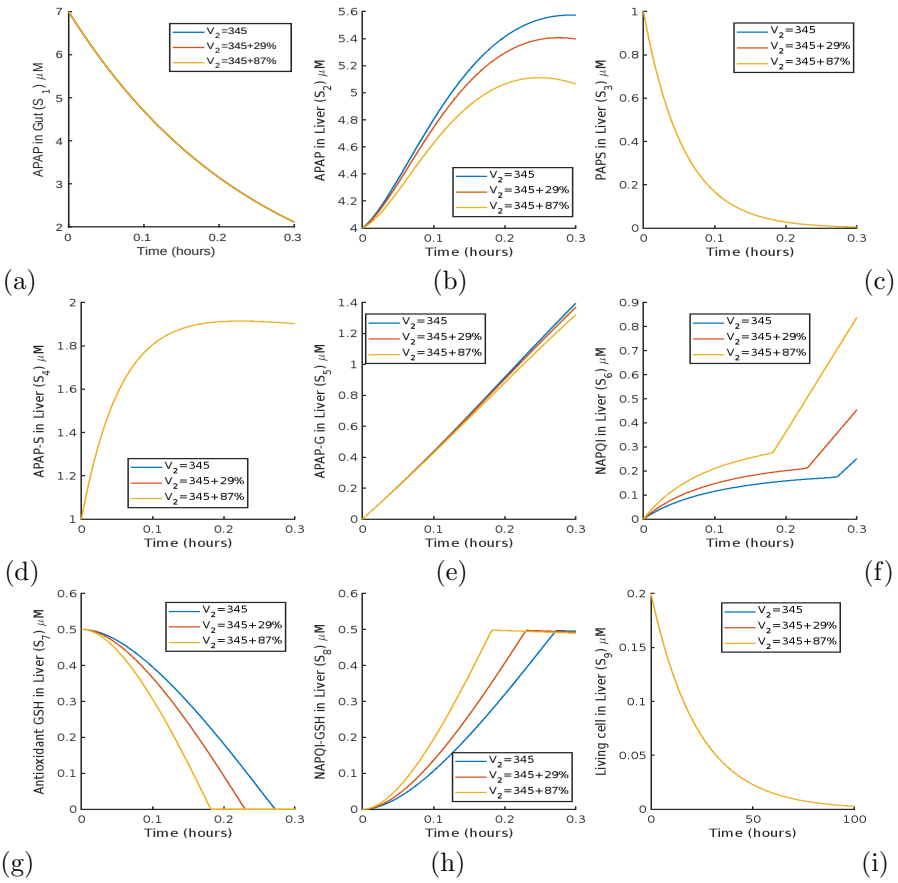

Figure 3. Concentrations for varying levels of maximum CYP rate (V_2): (a) APAP-G concentration in the liver function organ; (b) NAPQI concentration in the liver; and (c) antioxidant GSH concentration in the liver.

detoxification process by conjugating GSH with toxic compounds can be escalated and excreted via urine. The optimal control problem is numerically solved using the Steepest Descent method [43] with zero initial guesses. Runge Kutta's forward and backward methods [31] are used for solving the state and costate variables. Table 5 shows simulation results for different cases of objective weight. The results show the percentage of total concentration changes for all metabolites to the changes in the objective weight. The first case focuses on maximizing the GSH concentration where the highest weight is set for ξ_1. The optimal results show the highest percentage of changes occur on the total concentration of GSH that increases about 15.67% after regulation (see column 2 in Table 5). This affects NAPQI and NAPQI-GSH concentrations, which decrease by about 37.14% and 18.77%, respectively. In another case, for instance, case IV, the objective weights are set higher for ξ_2 and ξ_3, indicating that the optimization process is concerned with regulating both enzymes CYP and UGT simultaneously.

Compared to case I, the results of case IV show a more tremendous increase in GSH and a more significant decrease in NAPQI. If the weights of the three objectives are set almost equal, a considerable increase in GSH and NAPQI is obtained, but not

as great as the increase in case IV. Suppose the acetaminophen consumed is expected to be directly excreted in the form of urine without having to be bound by GSH. In that case, the concentration of APAP-G must be optimized. Therefore, among all cases, case I is the most recommended case because the total concentration of APAP-G increases by 0.49% (the highest concentration of APAP-G). However, if GSH increase rate and NAPQI decrease rate are considered then the best regulation is case IV, with GSH increasing by 52.23% and NAPQI decreasing by 69.90%. On the other hand, there is a case with different weights that results in an increase in APAP-G and GSH and a decrease in NAPQI. In this case, both excretion pathways can be optimized, but the increase in APAP-G is not as significant as in case I, and the increase in GSH and decrease in NAPQI are not as great as in case IV, as shown in Table 5.

Table 5. Change in value without control and with control with different cases and weights.

	Percentage of total concentration changes (%)				
	Case I ($\xi_1 = 80$ $, \xi_2 = 10, \xi_3 = 10$)	**Case II** ($\xi_1 = 10$ $, \xi_2 = 80, \xi_3 = 10$)	**Case III** ($\xi_1 = 10$ $, \xi_2 = 10, \xi_3 = 80$)	**Case IV** ($\xi_1 = 10$ $, \xi_2 = 45, \xi_3 = 45$)	**Case V** ($\xi_1 = 45$ $, \xi_2 = 10, \xi_3 = 45$)
S_1	- 1.53×10^{-6}	- 1.53×10^{-9}	9.32×10^{-6}	- 1×10^{-5}	- 5.08×10^{-7}
S_2	1.75	0.2	3.74	7.56	3.33
S_3	- 0.004	- 0.0004	0.003	- 0.04	- 0.002
S_4	0.0004	4.64×10^{-5}	- 0.0004	0.004	0.0002
S_5	0.49	0.049	- 0.43	- 19.82	0.19
S_6	- 37.14	- 5.36	- 60.79	- 69.90	- 57.52
S_7	15.67	1.26	38.48	52.23	34.23
S_8	- 18.77	- 1.51	- 45.98	- 62.27	- 40.92
S_9	6.44×10^{-6}	7.58×10^{-7}	1.5×10^{-5}	2.01×10^{-5}	1.34×10^{-5}

Case V, with the weights $\xi_1 = \xi_3 = 45$ and $\xi_2 = 10$, focuses more on maximizing the concentration of GSH (S_7) and UGT (u_2), but is less focused on minimizing the reaction rate of CYP (u_1). This condition is optimal because NAPQI can be completely bound when antioxidant production increases. When the production of UGT enzymes increases, the metabolic output in this pathway is greater, so this process helps reduce the toxicity of APAP in the liver. Case V also favors in reducing the productivity of CYP enzymes. Case V effectively increases the production of antioxidant GSH and UGT enzymes, which are important for reducing APAP toxicity by increasing glucuronide conjugation. Meanwhile, the focal reduction in CYP enzymes supports the decrease of NAPQI metabolite formation, making these conditions optimal for minimizing liver damage due to APAP toxicity.

Numerical simulations in Figure 4 show that the optimally applied control in cases I-V regulation can significantly reduce the hepatotoxicity effect of acetaminophen within 18 minutes after drug use. Among all metabolites, CYP and UGT regulation notably affects the concentrations of APAP-U in the gut, PAPS in the liver, APAP-S in the liver, and living cells (see Figure 4-(a,c,d,i)). However, prioritizing the weight towards S_7 can increase the concentration of APAP-L, APAP-G, and GSH by 1.75%, 0.49%, and 15.67%, respectively. As a result, the concentration of NAPQI and NAPQI-GSH complex decreases by 37.14% and 18.77%, respectively (see Figure 4-(b,e,f,g,h)). In addition, Figure 5-(a) shows that the maximum application of inhibiting CYP enzyme (u_1) at the 9th minute and UGT enzyme (u_2) at the 12th minute after drug use is an effective control strategy to manage he-

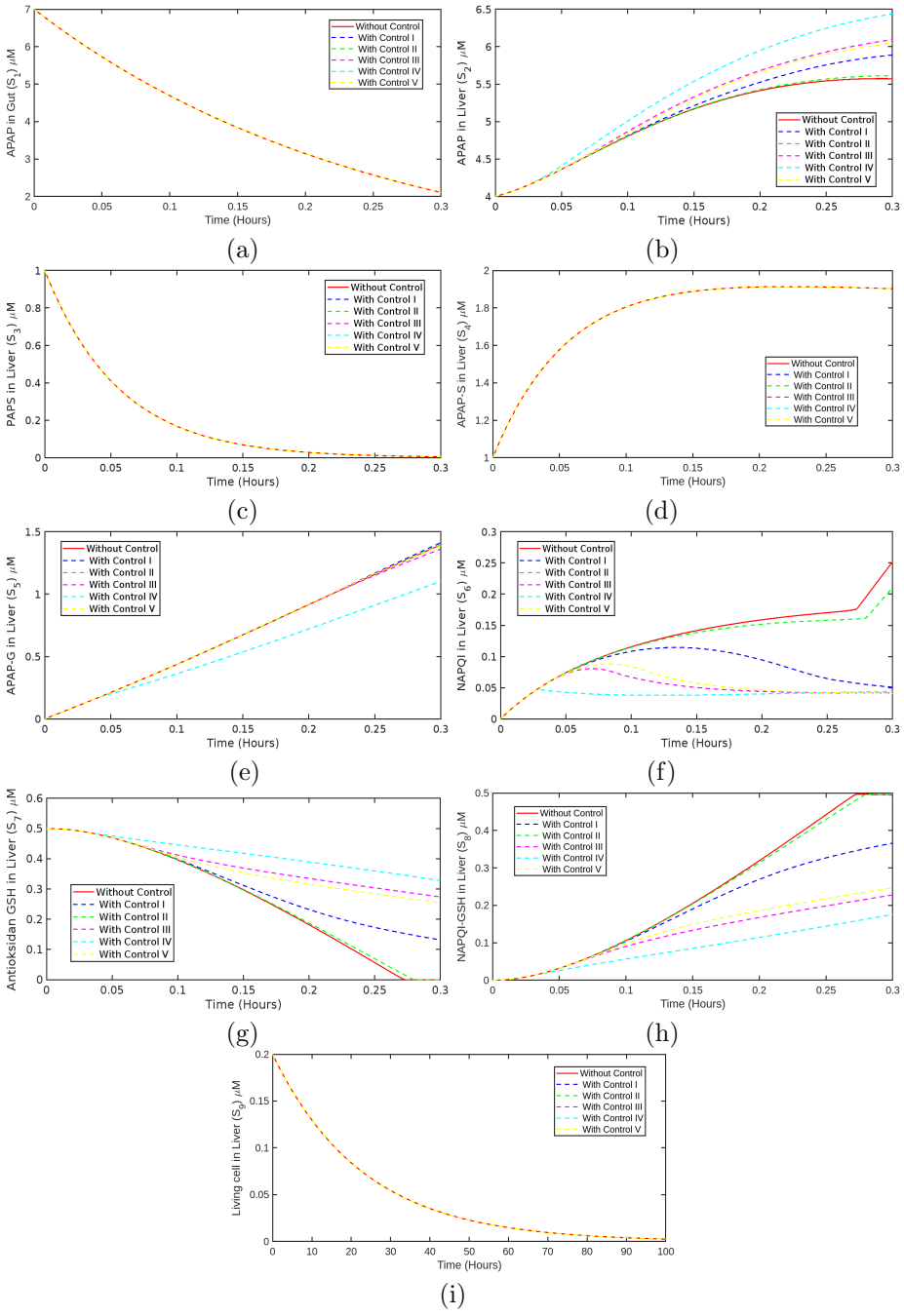

Figure 4. Numerical simulation for overdose condition without control (solid line) and using control (dashed line). The graphs show the dynamic of: (a) APAP Concentration in Gut, (b) APAP Concentration in Liver function organ, (c) PAPS Concentration in Liver function organ, (d) APAP-S Concentration in Liver function organ, (e) APAP-G Concentration in Liver function organ, (f) NAPQI Concentration in Liver function organ, (g) Antioxidant GSH in Liver function organ, (h) NAPQI GSH Concentration in Liver function organ, (i) Living Cell.

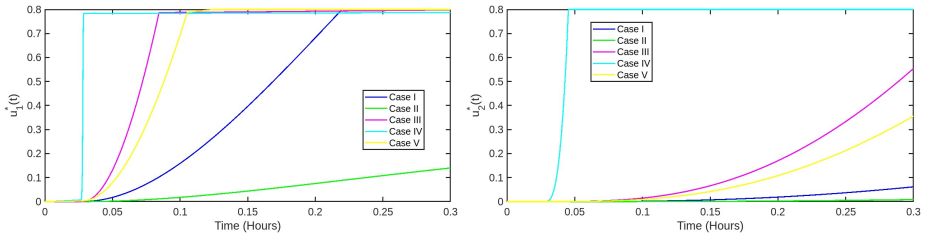

Figure 5. Comparison of optimal control functions with regulations of; (a) CYP u_1^*, (b) UGT u_2^*

patotoxicity. In this case, the expected acetaminophen concentration consumed is directly eliminated in urine without being bound by GSH. Hence, the concentration of APAP-G is optimized.

Numerical simulations in Figure 4 show that the optimally applied control in case IV regulation significantly reduces the hepatotoxicity effect of acetaminophen within 18 minutes after drug use. Among all metabolites, CYP regulation significantly affects the concentrations of APAP-L in the liver, APAP-G in the liver, NAPQI, GSH, and NAPQI-GSH complex (see Figure 4-(b,e,f,g,h)). However, by prioritizing the weights on enzymatic CYP (u_1) and enzymatic UGT (u_2), the concentration of GSH increased by 52.23%. In contrast, the concentrations of APAP-G, NAPQI complex, and NAPQI-GSH decreased by 19.82%, 69.90%, and 62.27%, respectively (see Figure 4-(b,e,f,g,h)). For other metabolites, the regulation did not have a significant effect (see Figure 4-(a,c,d,i)). In addition, Figure 5-(b) shows that the maximum application of inhibiting CYP enzymes (u_1) and UGT enzymes (u_2) at nearly the same time, i.e., the first minute after drug use is an effective control strategy to manage hepatotoxicity. This case makes antioxidants more likely to bind NAPQI so they can be excreted into the urine.

In case V, regulation showed that the optimally applied control significantly reduced the hepatotoxicity effect of acetaminophen within 18 minutes after drug use (see Figure 4). Among all metabolites, CYP regulation significantly affected the concentrations of APAP-L in the liver, NAPQI, GSH, and NAPQI-GSH complex (see Figure 4-(b,f,g,h)). However, by prioritizing the weights on GSH concentration (S_7) and enzymatic UGT (u_2), GSH concentration increased by 34.23%. At the same time, NAPQI and NAPQI-GSH complexes decreased by 57.52% and 40.92%, respectively (see Figure 4-(b,f,g,h)). For other metabolites, the regulation did not have a significant effect, but there was an increase in APAP-G by 0.19% (see Figure 4-(a,c,e,d,i)). In addition, Figure 5-(c) shows the maximum application of inhibiting CYP enzyme (u_1) in the first minute after drug application and UGT enzyme (u_2) in the third minute after drug application and gradually. This case produces a high enough concentration of antioxidants to bind NAPQI to be excreted into the urine, and metabolic products are disposed via the glucuronidation pathway (APAP-G) process.

In summarizy, based on our results, we found the two best regulation keys through sensitivity analysis using metabolic control analysis. This finding is in line with the study of [32], which stated that isoniazid can inhibit the concentration of CYP enzymes, thereby reducing APAP oxidation. In addition, [33] also found that increasing the concentration of UGT enzymes helps in conjugation and excretion. We then applied these two regulatory keys in the control theory to reduce the effects

of hepatotoxicity caused by acetaminophen metabolism.

6. Conclusion

We have generated a kinetic model for acetaminophen metabolism based on the properties of the enzymes with unimolecular and bimolecular Michaelis-Menten kinetics. The model focuses on the acetaminophen metabolism in the liver, consisting of three major pathways, i.e., cytochrome, sulfation, and glucuronidation. Metabolic regulation was studied by combining kinetic modeling, metabolic control analysis, and optimal control approaches to determine the optimal regulation for enzymes to regulate the metabolic process. It was found that the change in NAPQI concentration is highly controlled by the input rate of the APAP from the gut to the liver. On the other hand, to increase or decrease the concentration of APAP-G and GSH, which can help reduce the NAPQI concentration, reactions by CYP and UGT are the most recommended to be regulated. By inhibiting the maximum rate of CYP and increasing the concentration of GSH, the concentration of APAP-G can be increased such that APAP-L can be directly excreted through urine and the formation of toxic compounds (NAPQI) can be reduced. When we simultaneously minimize the maximum reaction rates of CYP and UGT, this reduces the concentration of NAPQI and increases the concentration of GSH, forming a NAPQI-GSH complex that is excreted in the urine. This result can then be used as guidance to explore the limits of metabolic regulation involving order-of-magnitude changes in the CYP and UGT activities such that a temporarily stable and optimal metabolic system can be maintained and the toxic effects of acetaminophen overdose can be reduced.

Acknowledgment

We thank the anonymous reviewers for their valuable comments and suggestions.

Use of AI tools declaration

The authors declare they have not used Artificial Intelligence (AI) tools in creating this article.

References

[1] Ramachandran, A., and Jaeschke, H, *Acetaminophen Hepatotoxicity,* Seminars in liver disease, **39(2)**, pp. 221–234, 2019. https://doi.org/10.1055/s-0039-1679919.

[2] Sankarraman, S. M, *A computational approach on acetaminophen drug using degree-based topological indices and m-polynomials,* Biointerface Research in Applied Chemistry, **12(6)**, pp. 7249–7266, 2022. https://doi.org/10.33263/BRIAC126.72497266.

[3] Yoo, SH., Lee, SC. and Kim, SB, *Acetaminophen adsorption to spherical carbons hydrothermally synthesized from sucrose: experimental, molecular, and mathematical modeling studies,* Environ Sci Pollut Res, **30**, pp. 49703–49719,

2023.
https://doi.org/10.1007/s11356-023-25815-x.

[4] Ghosh, A., Berger, I., Remien, C. H., and Mubayi, A., *The role of alcohol consumption on acetaminophen induced liver injury: Implications from a mathematical model,* Journal of theoretical biology, **519**, 110559,2021.
https://doi.org/10.1016/j.jtbi.2020.110559.

[5] Cairns, R., Brown, J. A., Wylie, C. E., Dawson, A. H., Isbister, G. K., and Buckley, N. A, *Paracetamol Poisoning-Related Hospital Admissions and Deaths in Australia, 2004-2017,* Medical Journal of Australia, **211(5)**, pp. 218–223, 2019.
https://doi.org/10.5694/mja2.50296.

[6] Bateman, D. N., Carroll, R., Pettie, J., Yamamoto, T., Elamin, M. E., Peart, L., Dow, M., Coyle, J., Cranfield, K. R., Hook, C., Sandilands, E. A., Veiraiah, A., Webb, D., Gray, A., Dargan, P. I., Wood, D. M., Thomas, S. H., Dear, J. W., and Eddleston, M, *Effect of the UK's revised paracetamol poisoning management guidelines on admissions*, Adverse reactions and costs of treatment, **78(3)**, pp. 610–618, 2014.
https://doi.org/10.1111/bcp.12362.

[7] Reed, M. C., Thomas, R. L., Pavisic, J., James, S. J., Ulrich, C. M., and Nijhout, H. F, *A mathematical model of glutathione metabolism,* Theoretical biology and medical modelling, **5**, 8, 2008.
https://doi.org/10.1186/1742-4682-5-8.

[8] Reith, D., Medlicott, N. J., Silva, R. K. D., Yang, L., Hickling, J., and Zacharias, M, *Simultaneous Modelling of the Michaelis-Menten Kinetics of Paracetamol sulfate and Glucuronidation,* Clinical and Experimental Pharmacology and Physiology, pp. 35–42, 2009.
https://doi.org/10.1111/j.1440-1681.2008.05029.

[9] Ben-Shachar, R., Chen, Y., Luo, S., Hartman, C., Reed, M., and Nijhout, H. F, *The biochemistry of acetaminophen hepatotoxicity and rescue: a mathematical model,* Theoretical biology and medical modelling, 9, 55, 2012.
https://doi.org/10.1186/1742-4682-9-55.

[10] Remien, C. H., Adler, F. R., Waddoups, L., Box, T. D., and Sussman, N. L, *Mathematical modeling of liver injury and dysfunction after acetaminophen overdose: early discrimination between survival and death,* Hepatology (Baltimore, Md.**56(2)**, pp. 727–734, 2012.
https://doi.org/10.1002/hep.25656.

[11] Reddyhoff, D., Ward, J., Williams, D., Regan, S., and Webb, S, *Timescale analysis of a mathematical model of acetaminophen metabolism and toxicity,* Journal of theoretical biology, **386**, pp. 132–146, 2015.
https://doi.org/10.1016/j.jtbi.2015.08.021.

[12] Gilman, G, *In The Pharmacological Basic of Therapeutic,* Unites States of America: Mc Graw-Hill, 2006.

[13] Katzung, B. G., Masters, S. B., and Trevor, A. J, *Basic and clinical pharmacology*, 2004.

[14] Hinson, J. A., Roberts, D. W., and James, L. P., *Mechanisms of acetaminophen-induced liver necrosis,* Handbook of experimental pharmacol-

ogy, **(196)**, pp. 369–405, 2010.
https://doi.org/10.1007/978-3-642-00663-0_12.

[15] Campbell and Reece, *Biology ed VIII, Jakarta: Erlangga*, 2008.

[16] Wang, Xinxin and Wang, Xiaoyun, *Optimal Control of a Fractional-Order New Psychoactive Substance Model,* Journal of Nonlinear Modeling and Analysis, **6(3)**, pp. 573–588, 2024.
doi:10.12150/jnma.2024.573.

[17] Ingalls, B. P, *Mathematical modeling in systems biology: an introduction,* MIT press, 2013.

[18] Dichamp, J., Cellière, G., Ghallab, A., Hassan, R., Boissier, N., Hofmann, U., Reinders, J., Sezgin, S., Zühlke, S., Hengstler, J. G., and Drasdo, D., *In vitro to in vivo acetaminophen hepatotoxicity extrapolation using classical schemes, pharmacodynamic models and a multiscale spatial-temporal liver twin,* Frontiers in bioengineering and biotechnology, **(11)**, 2023.
https://doi.org/10.3389/fbioe.2023.1049564.

[19] Craig, D. G. N., Bates, C. M., Davidson, J. S., Martin, K. G., Hayes, P. C., and Simpson, K. J, *Staggered Overdose Pattern and Delay to Hospital Presentation are Associated with Adverse Outcomes Following Paracetamol-Induced Hepatotoxicity,* British Journal of Clinical Pharmacology, **73(2)**, pp. 285–294, 2012.
https://doi.org/10.1111/j.1365-2125.2011.04067.

[20] Meiss, J. D, *Differential Dynamical Systems,* USA: SIAM, 2007.

[21] Nayfeh, A. H, *Nonlinear Oscillations,* John Wiley and Sons, 2008.

[22] Castillo-Chavez C, Song B, *Dynamical models of tuberculosis and their applications,* Math. Biosci.Eng., **1**, 361–404, 2004.
https://dx.doi.org/10.3934/mbe.2004.1.361.

[23] Murray, J, *Mathematical Biology: I. An Introduction,* New York: Springer-Verlag, 2001.

[24] Olsder, and Woude, *Mathematical System Theory, 2nd Edition,* Netherlands: Delft University of Technology, 2003.

[25] Frank J. Bruggeman, Maaike Remeijer, Maarten Droste, Luis Salinas, Meike Wortel, Robert Planqué, Herbert M. Sauro, Bas Teusink, Hans V. Westerhoff, *Whole-cell metabolic control analysis,* Biosystems, **234**, 2023.
https://doi.org/10.1016/j.biosystems.2023.105067.

[26] Kasbawati, Gunawan, A. Y., Hertadi, R., and Sidarto, K. A, *Metabolic regulation and maximal reaction optimization in the central metabolism of a yeast cell,* In Symposium on Biomathematics (SYMOMATH 2014) (1651) 1, pp. 75–85, American Institute of Physics, 2015, March.
https://doi.org/10.1063/1.4914436.

[27] Palsson, B, *Systems Biology: Properties of Reconstructed Network,* Cambridge University Press, 2006.

[28] Trinh, C. T., Wlaschin, A., and Srienc, F, *Elementary mode analysis: a useful metabolic pathway analysis tool for characterizing cellular metabolism,* Applied microbiology and biotechnology, **81(5)**, pp. 813–826, 2009.
https://doi.org/10.1007/s00253-008-1770-1.

[29] Hofmeyr, J., Hucka, M., Morohashi, M., and Kitano, H, *Metabolic control analysis in a nutshell*, 2001.

[30] Belmont-Díaz, J., Vázquez, C., Encalada, R., Moreno-Sánchez, R., Michels, P.A.M., Saavedra, E, *Metabolic Control Analysis for Drug Target Selection Against Human Diseases*. In: Springer, Cham, **1**, 2022. https://doi.org/10.1007/978-3-030-95895-4$_8$.

[31] Lenhart, S., and Workman, J, *Optimal Control Applied to Biological Models,* Francis: CRC Press, 2007.

[32] Wen, X., Wang, J. S., Neuvonen, P. J., and Backman, J. T, *Isoniazid is a mechanism-based inhibitor of cytochrome P450 1A2, 2A6, 2C19 and 3A4 isoforms in human liver microsomes,* European journal of clinical pharmacology, **57(11)**, pp. 799–804, 2002. https://doi.org/10.1007/s00228-001-0396-3.

[33] Mazaleuskaya, L. L., Sangkuhl, K., Thorn, C. F., FitzGerald, G. A., Altman, R. B., and Klein, T. E, *PharmGKB summary: pathways of acetaminophen metabolism at the therapeutic versus toxic doses,* Pharmacogenetics and genomics, **25(8)**, pp. 416–426, 2015. https://doi.org/10.1097/FPC.0000000000000150.

[34] Aw, T. Y., Ookhtens, M., Ren, C., and Kaplowitz, N. *Kinetics of glutathione efflux from isolated rat hepatocytes,* The American journal of physiology, **250(2 Pt 1)**, G236–G243, 1986. https://doi.org/10.1152/apngi.1986.250.2.G236.

[35] Kraus P. Resolution, *Purification and some properties of three glutathione transferases from rat liver mitochondria,* Hoppe-Seyler's Zeitschrift fur physiologische Chemie, **361(1)**, 9–15, 1980. https://doi.org/10.1515/bchm2.1980.361.1.9.

[36] Lauterburg, B.H., Adams, J.D. and Mitchell, J.R, *Hepatic Glutathione Homeostasis in the Rat: Efflux Accounts for Glutathione Turnover,* Hepatology, **4**, 586–590, 1984. https://doi.org/10.1002/hep.1840040402.

[37] Miner, D. J., and Kissinger, P. T, *Evidence for the involvement of N-acetyl-p- quinoneimine in acetaminophen metabolism,* Biochemical pharmacology, **28(22)**, 3285–3290, 1979. https://doi.org/10.1016/0006-2952(79)90123-0.

[38] Mutlib, A. E., Goosen, T. C., Bauman, J. N., Williams, J. A., Kulkarni, S., and Kostrubsky, S. *Kinetics of acetaminophen glucuronidation by UDP-glucuronosyltransferases 1A1, 1A6, 1A9 and 2B15. Potential implications in acetaminophen-induced hepatotoxicity,* Chemical research in toxicology, **19(5)**, 701–709, 2006. https://doi.org/10.1021/tx050317i.

[39] Nagar, S., Walther, S.E., and Blanchard, R.L, *Sulfotransferase (SULT) 1A1 Polymorphic Variants *1, *2, and *3 Are Associated with Altered Enzymatic Activity, Cellular Phenotype, and Protein Degradation,* Molecular Pharmacology, **69**, 2084–2092, 2006.

[40] Ookhtens, M., Hobdy, K., Corvasce, M. C., Aw, T. Y., and Kaplowitz, N, *Sinusoidal efflux of glutathione in the perfused rat liver. Evidence for a carrier-*

mediated process, The Journal of clinical investigation, **75(1)**, 258–265, 1985. https://doi.org/10.1172/JCI111682.

[41] Patten, C. J., Thomas, P. E., Guy, R. L., Lee, M., Gonzalez, F. J., Guengerich, F. P., and Yang, C. S, *Cytochrome P450 enzymes involved in acetaminophen activation by rat and human liver microsomes and their kinetics,* Chemical research in toxicology, **6(4)**, 511–518, 1993. https://doi.org/10.1021/tx00034a019.

[42] Pezzola, S., Antonini, G., Geroni, C., Beria, I., Colombo, M., Broggini, M., Marchini, S., Mongelli, N., Leboffe, L., MacArthur, R., Mozzi, A. F., Federici, G., and Caccuri, A. M, *Role of glutathione transferases in the mechanism of brostallicin activation,* Biochemistry, **49(1)**, 226–235, 2010. https://doi.org/10.1021/bi901689s.

[43] Daniilidis, A, Salas,D, *Steepest Geometric Descent for Regularized Quasiconvex Functions,* Set-Valued and Variational Analysis, **32(28)**, 2–20, 2024. https://doi.org/10.1007/s11228-024-00731-5.